Title: Correlations and topology in the magic angle twisted bilayer graphene

Speakers: Oskar Vafek
Date: February 08, 2021 - 12:30 PM

URL: http://pirsa.org/21020025

Abstract: When the twist angle of a bilayer graphene is near the ``magic" value, there are four narrow bands near the neutrality point, each two-fold spin degenerate. These bands are separated from the rest of the bands by energy gaps. In the first part of the talk, the topology of the narrow bands will be discussed, as well as the associated obstructions --or lack there of -- to construction of a complete localized basis [1,3].

In the second part of the talk, I will present a two stage renormalization group treatment [4] which connects the continuum Hamiltonian at length scales shorter than the moire superlattice period to the Hamiltonian for the active narrow bands only, which is valid at distances much longer than the moire period. Via a progressive numerical elimination of remote bands the relative strength of the one-particle-like dispersion and the interactions within the active narrow band Hamiltonian will be determined, thus quantifying the residual correlations and justifying the strong coupling approach in the final step.

In the last part of the talk, the states favored by electron-electron Coulomb interactions within the narrow bands will be discussed. Analytical and DMRG results based on 2D localized Wannier states [2,5], 1D localized hybrid Wannier states [3] and Bloch states [3,4] will be compared. Topological and symmetry constraints on the spectra of charged and neutral excitation[4] for various ground states, as well as non-Abelian braiding of Dirac nodes[3] , will also be presented.

[1] Jian Kang and Oskar Vafek, Phys. Rev. X 8, 031088 (2018).

[2] Jian Kang and Oskar Vafek, Phys. Rev. Lett. 122, 246401 (2019)

[3] Jian Kang and Oskar Vafek, Phys. Rev. B 102, 035161 (2020)

[4] Oskar Vafek and Jian Kang Phys. Rev. Lett. 125, 257602 (2020)

[5] Bin-Bin Chen, Yuan Da Liao, Ziyu Chen, Oskar Vafek, Jian Kang, Wei Li, Zi Yang Meng arXiv:2011.07602

Correlations and topology in the magic angle twisted bilayer graphene

Oskar Vafek

National High Magnetic Field Laboratory

and

Department of Physics, Florida State University, Tallahassee, FL

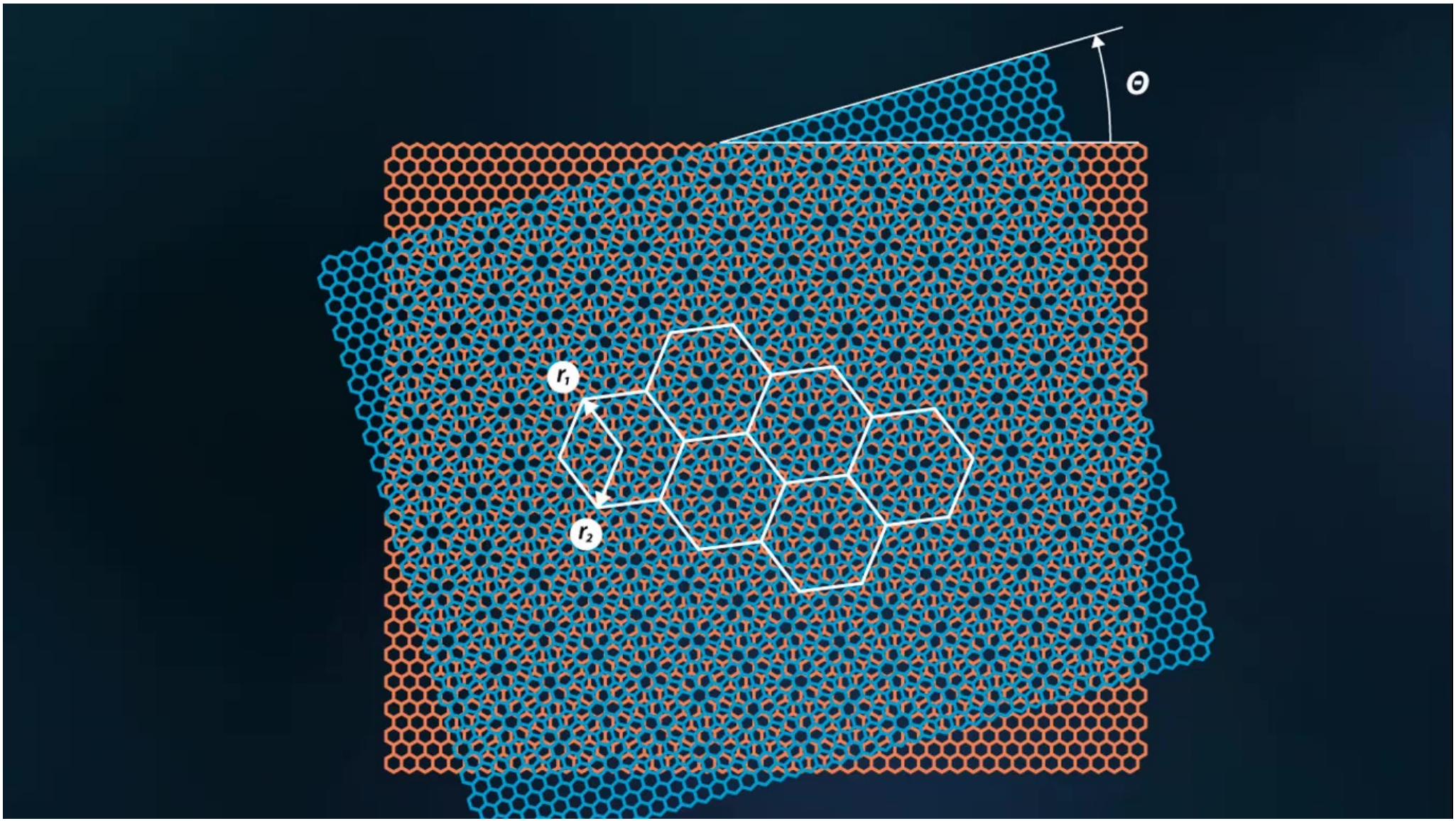
Θ
r_1
r_2

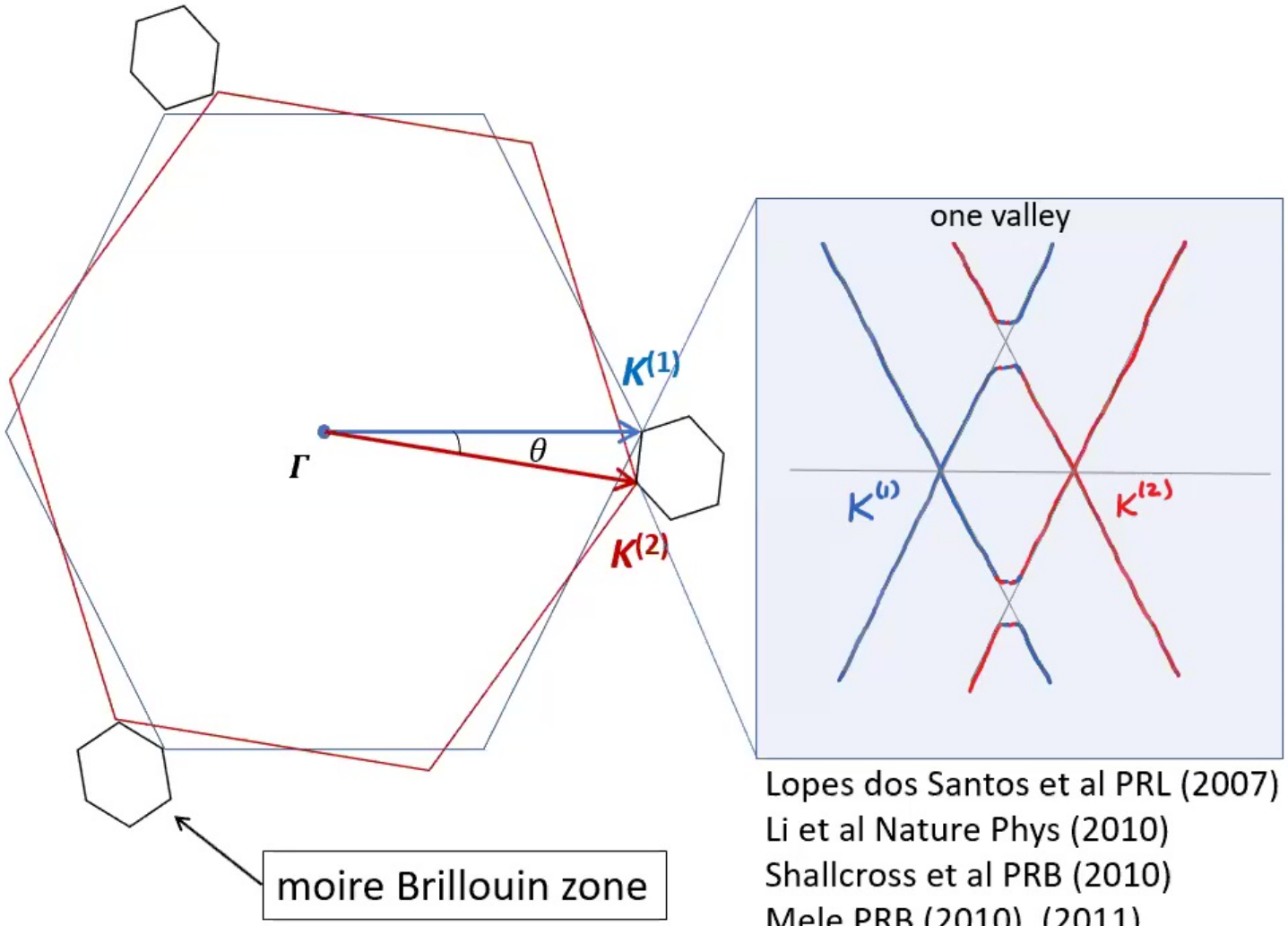

Lopes dos Santos et al PRL (2007)
Li et al Nature Phys (2010)
Shallcross et al PRB (2010)
Mele PRB (2010), (2011)
Bistritzer&MacDonald PNAS (2011)

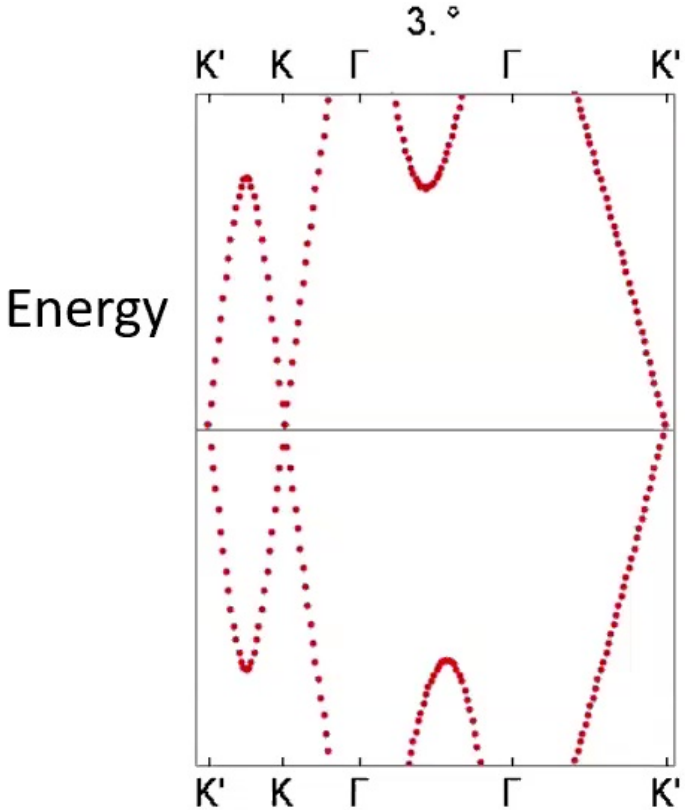

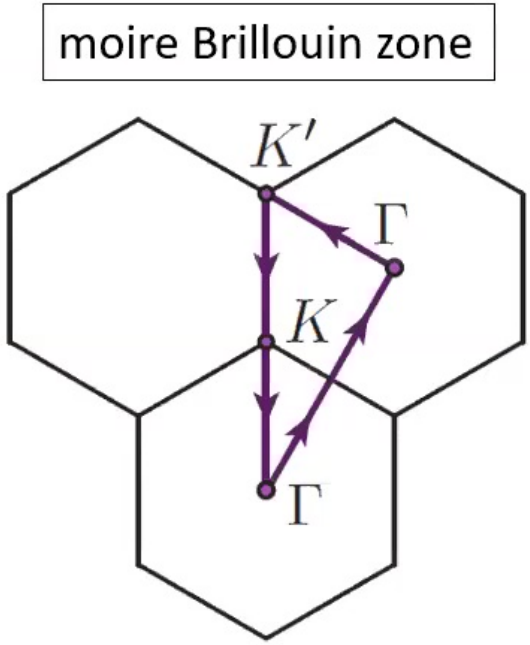

Bistritzer&MacDonald PNAS (2011)

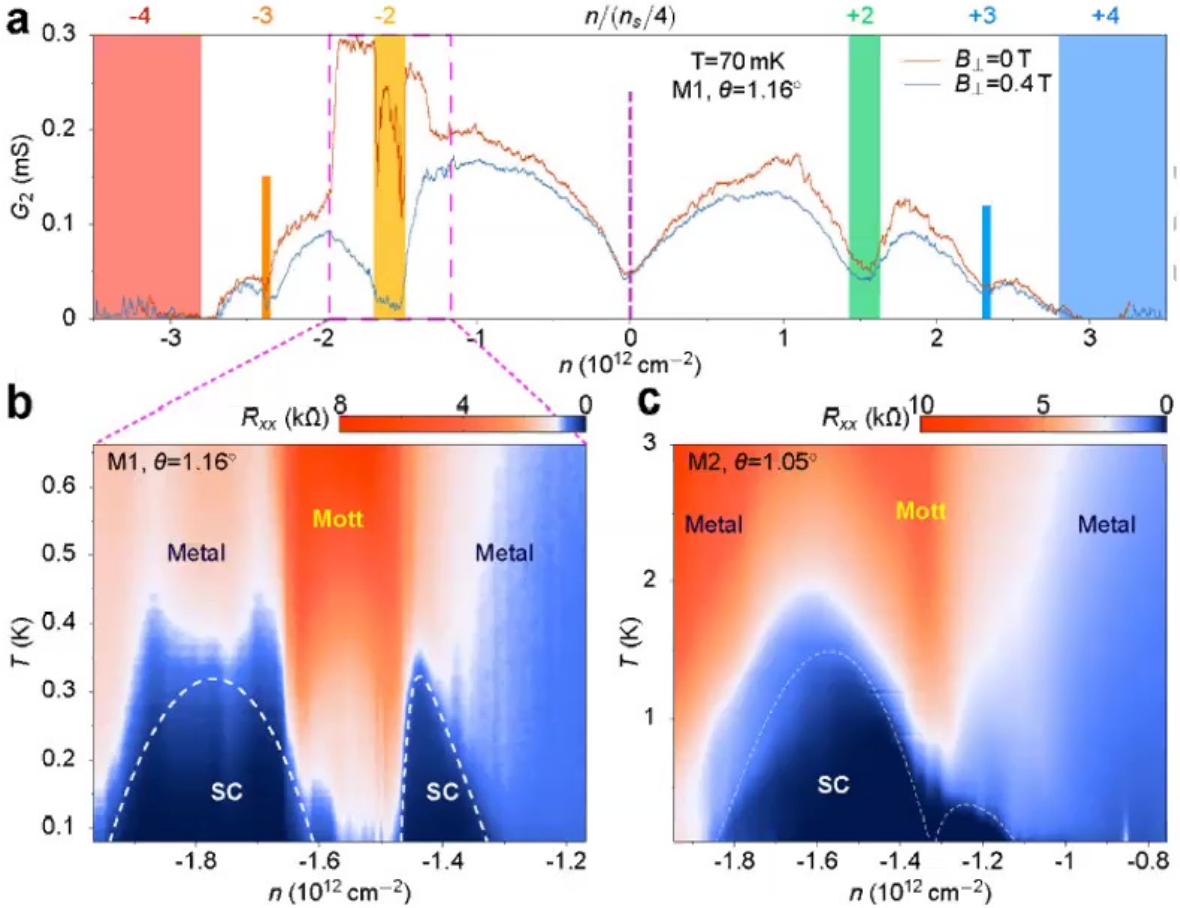

Yuan Cao *et al. Nature* **556**, 80 (2018)
Yuan Cao *et al. Nature* **556**, 43 (2018)

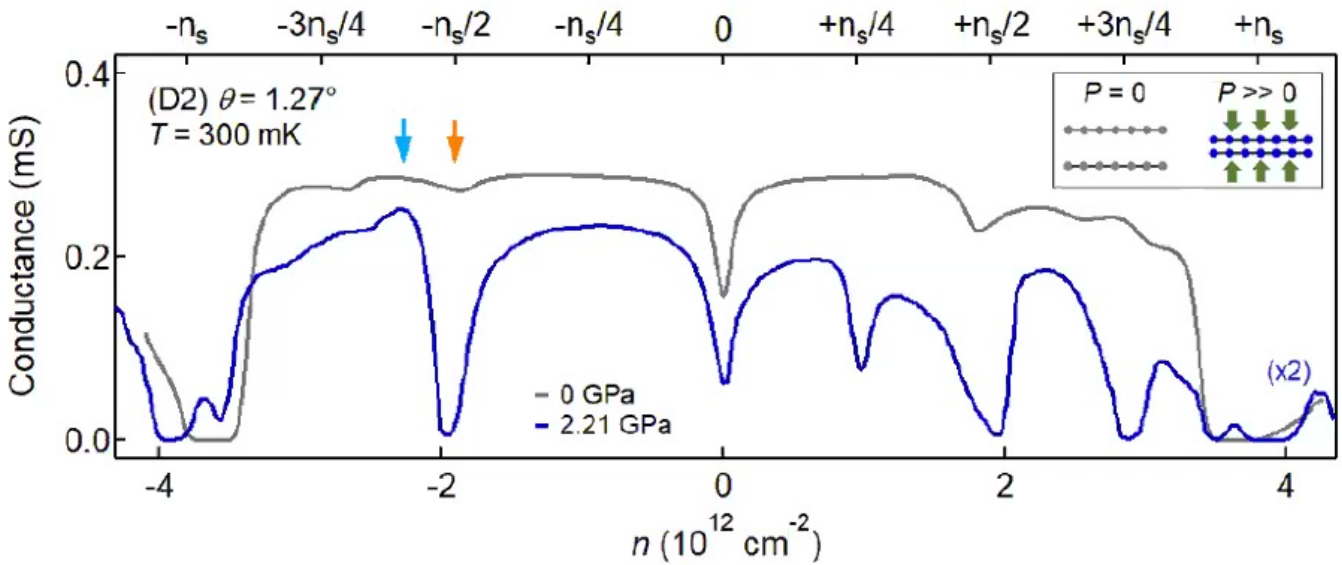

Yankowitz et al (Andrea Young, Cory Dean group) Science 2019

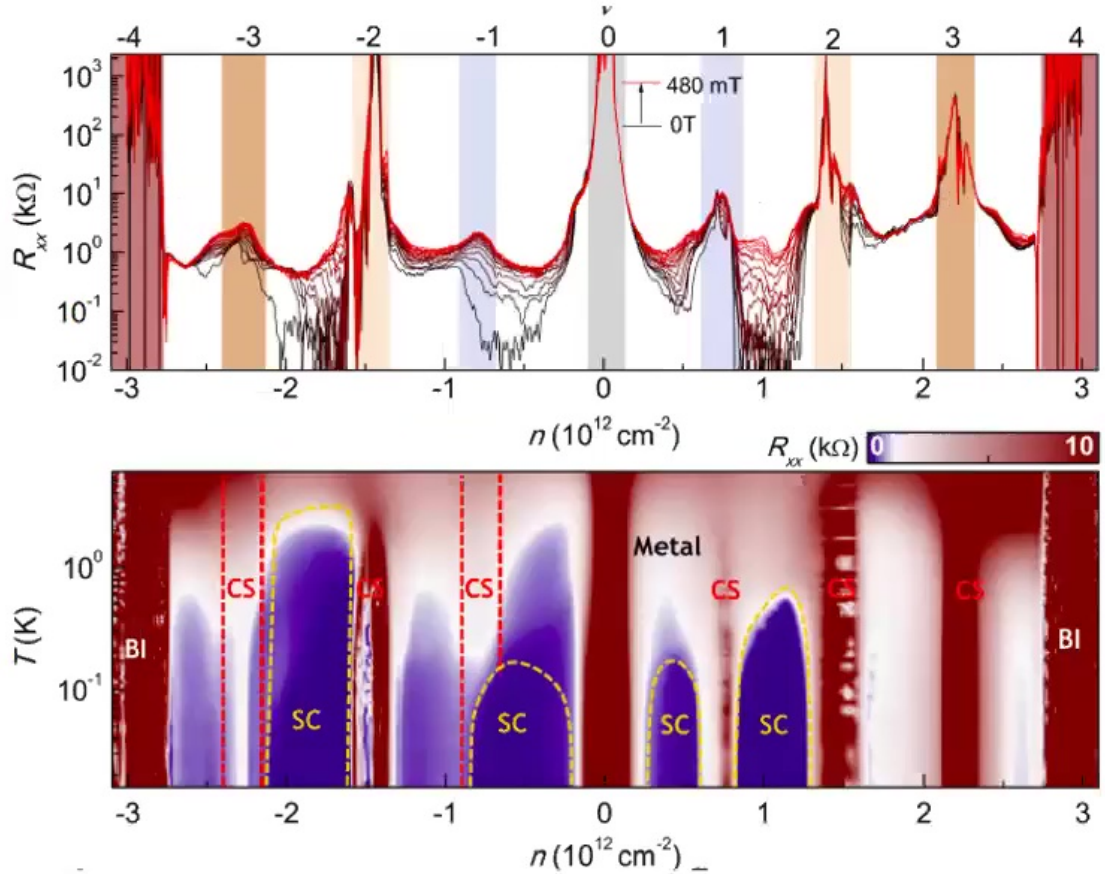

X. Lu et al Nature 2019 (D. K. Efetov group)

General considerations: insulation occurs at simple (integer) commensurate filling of the four bands

General considerations: insulation occurs at simple (integer) commensurate filling of the four bands

- Difficult to reconcile with the notion that the insulation is due to Fermi surface nesting, or the van Hove singularities, because such band structure features generically occur at *incommensurate* fillings.

- Fine-tuning with angle/pressure suggests that the effective Coulomb interaction dominates the effective kinetic energy.

- Even if the physical system is ultimately in an intermediate coupling regime, a strong coupling approach may be more successful in capturing the nature of the correlated phases. In this approach the interaction-only Hamiltonian is minimized first, and the kinetic energy term is then treated as a perturbation.

Outline

1. Topology of the narrow bands and its consequences:
   Wannier states (2D localized), hybrid Wannier states (1D localized) and smooth gauge Bloch states (extended)

2. Two Stage RG connecting the short distance physics to the physics of the narrow bands

3. Residual Coulomb interaction analyzed in different basis:
   - 2D Wannier – new form of lattice Hamiltonian: the usual anti-ferromagnetic super-exchange mechanism fails and turns ferromagnetic with an approximate spin-valley SU(4) symmetry;
     QAH and DMRG
   - 1D hybrid Wannier – DMRG, variational trial states for spinless one valley model: competition among Chern insulator, nematic and C_2T-stripe
   - smooth gauge Bloch basis – topology enforced gapless C_2T- nematic and gapped C_2T-stripe via non-Abelian Dirac node braiding

D_3 point group of the twisted bilayer with AA site registry

A pair of integers (m, n) defines the structure (and twist angle)

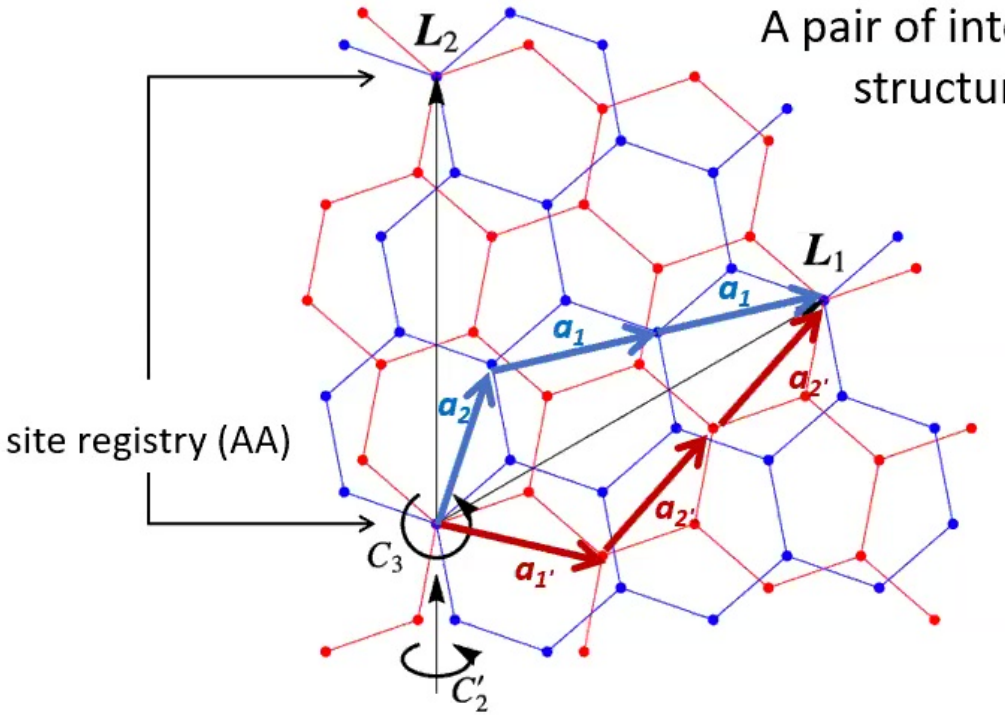

$n\, a_1 + m\, a_2 = m\, a_{1'} + n\, a_{2'}$

Note the absence of C_2'' and C_2T symmetry in the D_3 structure

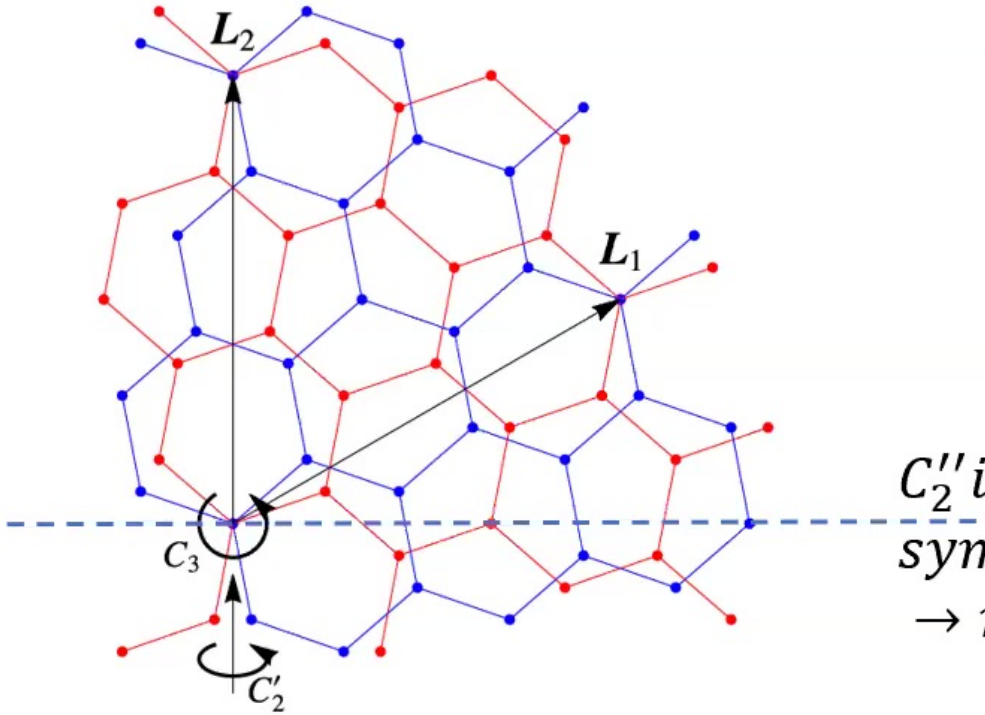

C_2'' $is\ not\ an\ exact\ symmetry$
$\rightarrow neither\ is\ C_2T.$

C_2'' *and* C_2T symmetries emerge at small angles

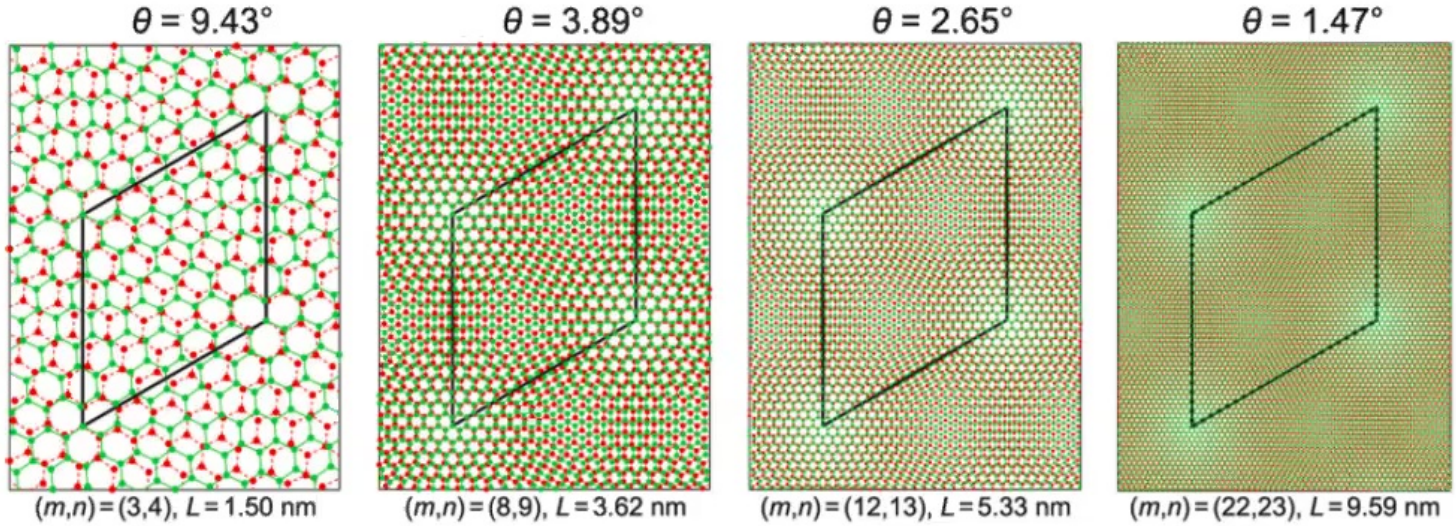

$$H = \sum_{\boldsymbol{R}_i, \boldsymbol{R}_j} t(\boldsymbol{R}_i - \boldsymbol{R}_j) c^\dagger_{\boldsymbol{R}_i} c_{\boldsymbol{R}_j} \ , \qquad \text{with} \quad t(\boldsymbol{d}) = -V_{pp\pi}\left[1 - \left(\frac{\boldsymbol{d}\cdot\boldsymbol{e}_z}{d}\right)^2\right] - V_{pp\sigma}\left(\frac{\boldsymbol{d}\cdot\boldsymbol{e}_z}{d}\right)^2$$

$$V_{pp\pi} = V^0_{pp\pi} \exp\left(-\frac{d - a_0}{\delta}\right) \qquad V_{pp\sigma} = V^0_{pp\sigma} \exp\left(-\frac{d - \boldsymbol{d}_0}{\delta}\right)$$

from Moon and Koshino PRB 85, 195458 (2012)

$(m, n) = (25,26) \qquad (\theta = 1.3^o)$

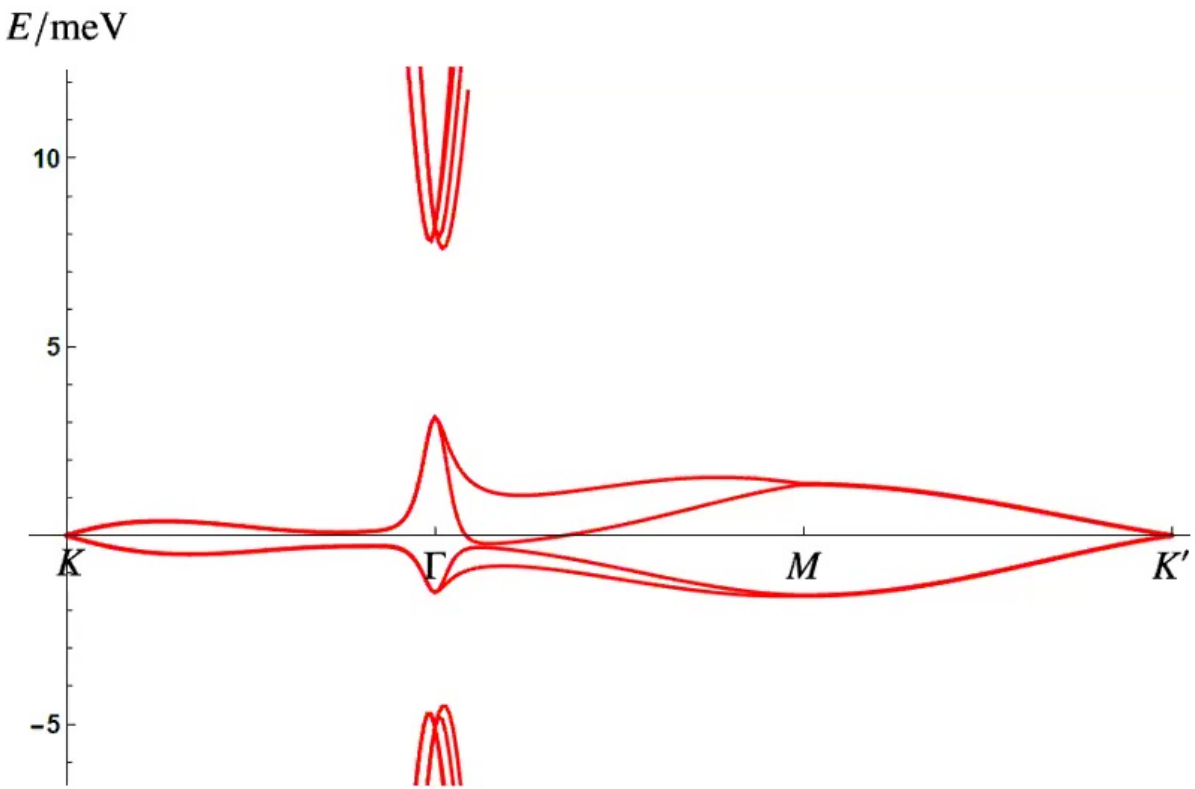

Jian Kang and OV PRX 8, 031088 (2018)

$(m, n) = (25,26) \qquad (\theta = 1.3^o)$

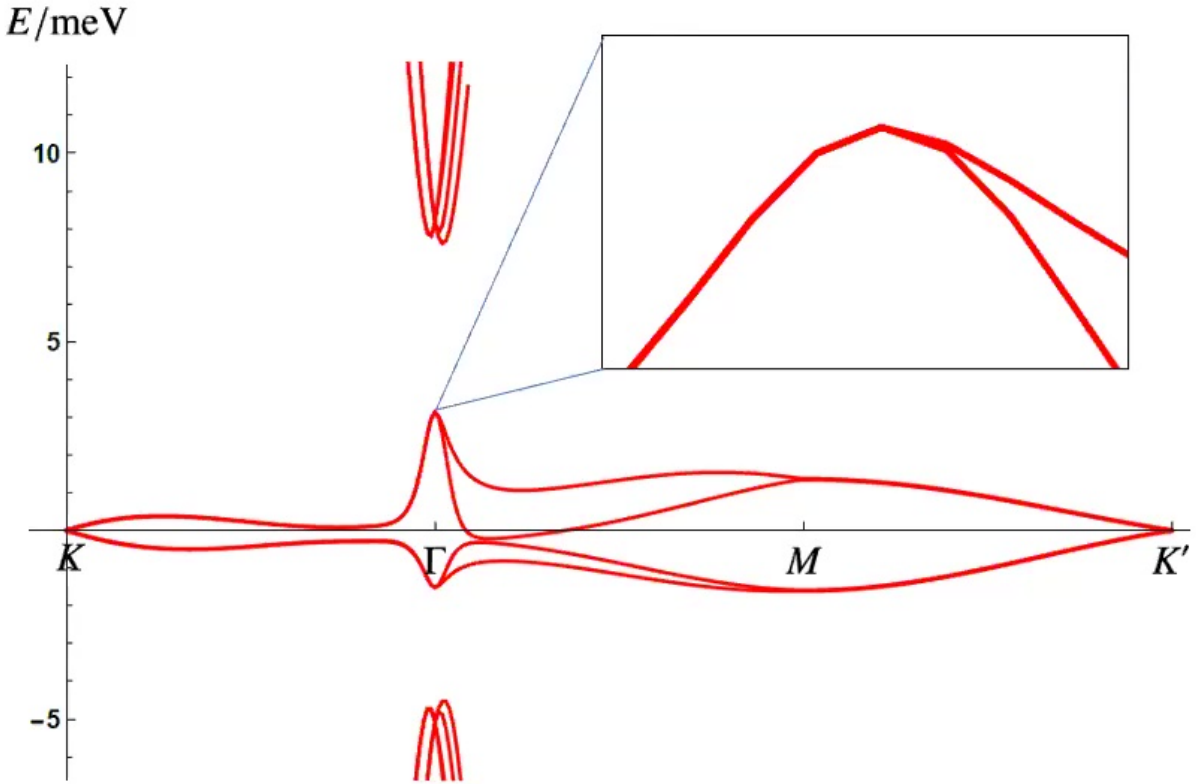

Jian Kang and OV PRX 8, 031088 (2018)

$(m, n) = (25,26) \qquad (\theta = 1.3^o)$

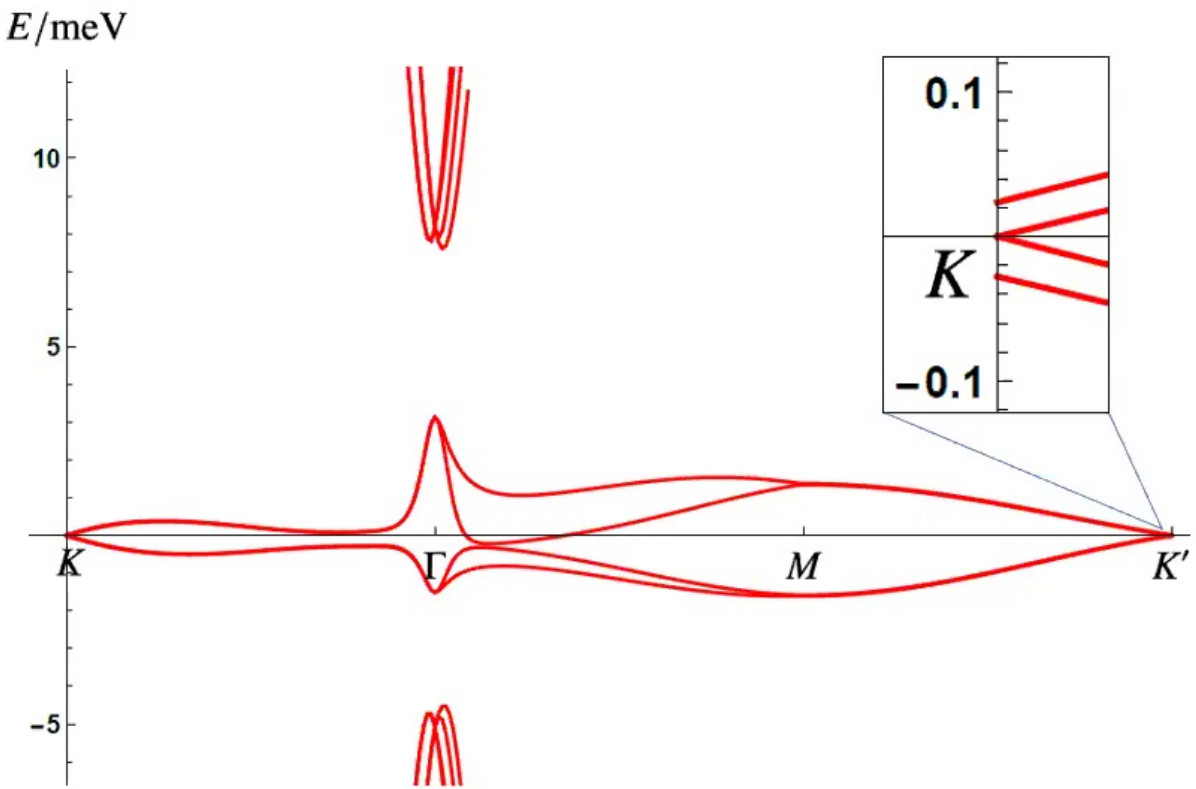

Jian Kang and OV PRX 8, 031088 (2018)

Local density of states (E>0): peaked at triangular moire sites

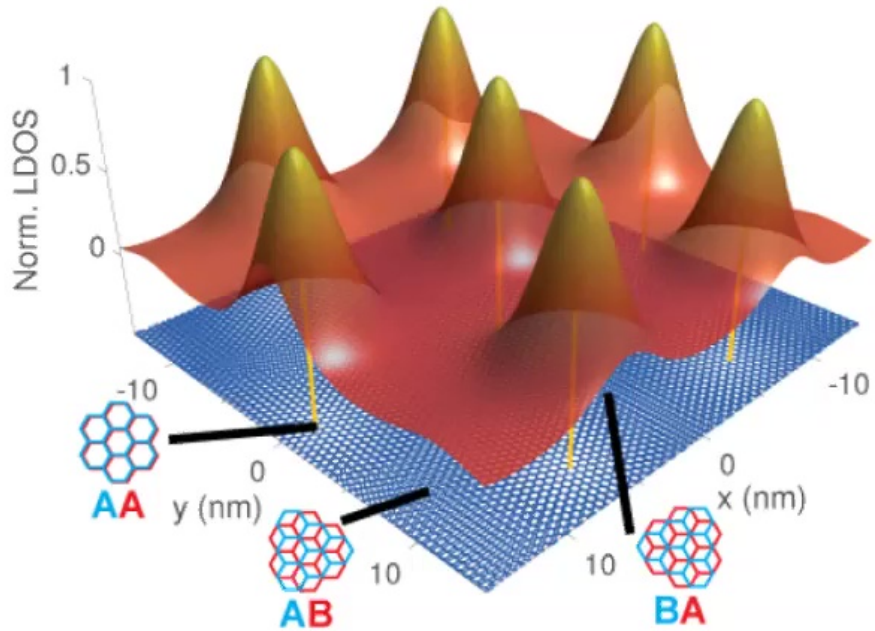

Yuan Cao *et al. Nature* **556**, 80 (2018)
Yuan Cao *et al. Nature* **556**, 43 (2018)

Wannier state centers: honeycomb moire sites

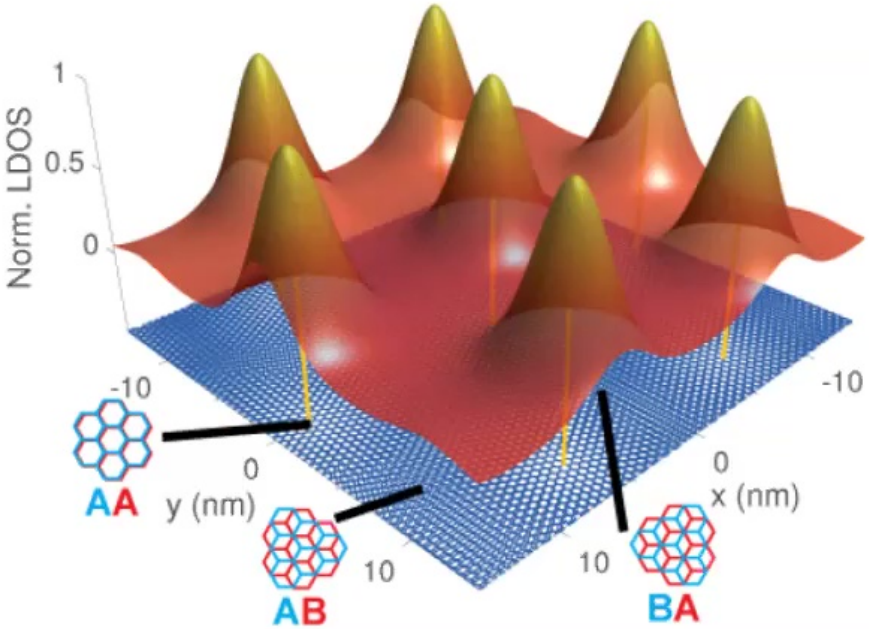

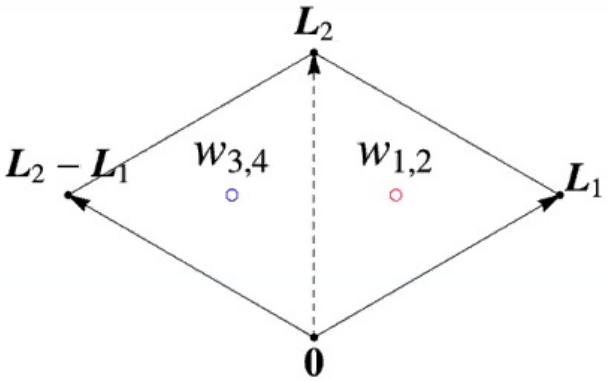

Yuan Cao *et al. Nature* **556**, 80 (2018)
Yuan Cao *et al. Nature* **556**, 43 (2018)

J. Kang and O. Vafek, PRX, 8, 031088 (2018)
See also:
Koshino et al. Phys. Rev. X **8**, 031087 (2018)
Hoi Chun Po et al. PRX **8**, 031089 (2018)

Advance to the next animation or slide

Wannier state centers: honeycomb moire sites

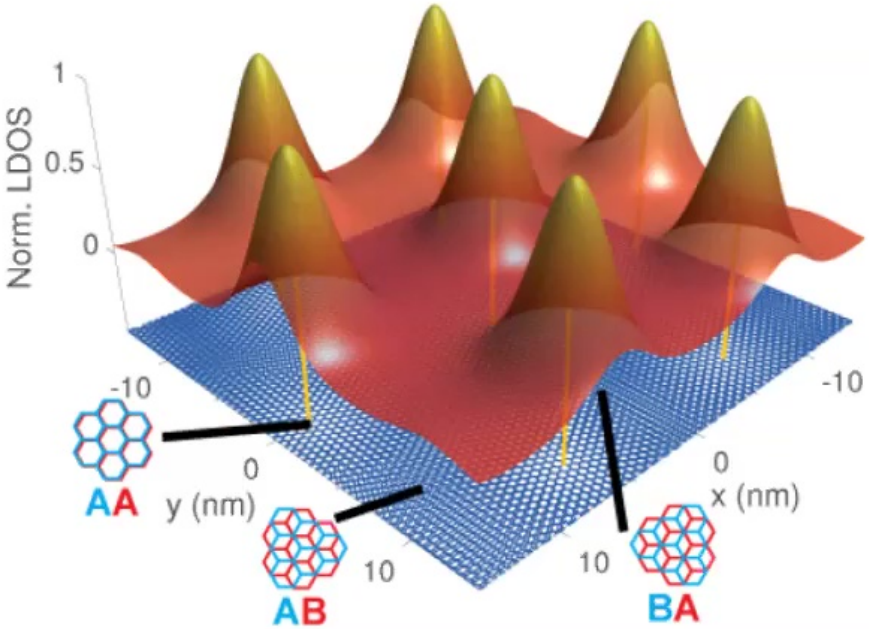

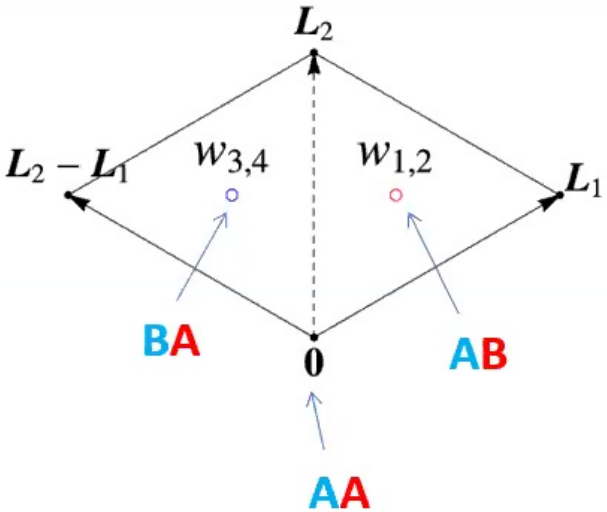

Yuan Cao *et al. Nature* **556**, 80 (2018)
Yuan Cao *et al. Nature* **556**, 43 (2018)

J. Kang and O. Vafek, PRX, 8, 031088 (2018)
See also:
Koshino et al. Phys. Rev. X **8**, 031087 (2018)
Hoi Chun Po et al. PRX **8**, 031089 (2018)

Maximally localized and D_3 symmetry adapted Wannier fxns

$$w_1$$
$$w_2 = w_1^*$$
$$w_3 = C_2' w_1$$
$$w_4 = w_3^*$$

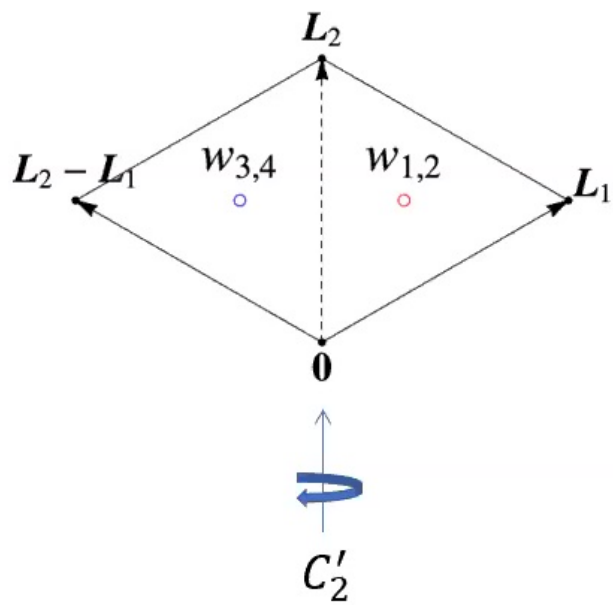

Jian Kang and OV PRX, 8, 031088 (2018)

Constructing Wannier functions

mixture of Bloch states, smooth in ***k***

For collection of isolated bands: $|w_{j,\boldsymbol{R}}\rangle = \int \frac{d^2\boldsymbol{k}}{(2\pi)^2} |\tilde{\psi}_{j,\boldsymbol{k}}\rangle e^{-i\boldsymbol{k}\cdot\boldsymbol{R}}$

smooth in ***k***

trial wannier fxn

$$|\phi_{i,\boldsymbol{k}}\rangle = \sum_j |\psi_{j,\boldsymbol{k}}\rangle\langle\psi_{j,\boldsymbol{k}}|g_i\rangle = \sum_j |\psi_{j,\boldsymbol{k}}\rangle A_{ji}(\boldsymbol{k})$$

ϕ is smooth in ***k*** (good for real space localization), but not orthonormal

$$|\tilde{\psi}_{i,\boldsymbol{k}}\rangle = \sum_j |\phi_{j,\boldsymbol{k}}\rangle S_{ji}^{-1/2}(\boldsymbol{k}) = \sum_j |\psi_{j,\boldsymbol{k}}\rangle \left(A(\boldsymbol{k})S^{-1/2}(\boldsymbol{k})\right)_{ji}$$

where

$$S(\boldsymbol{k}) = A^\dagger(\boldsymbol{k})A(\boldsymbol{k})$$

Marzari and Vanderbilt, PRB **56**, 12847 (1997)
Marzari et al. RMP **84**, 1419 (2012)

Maximally localized and symmetry adapted Wannier fxns

$|w_1|^2$

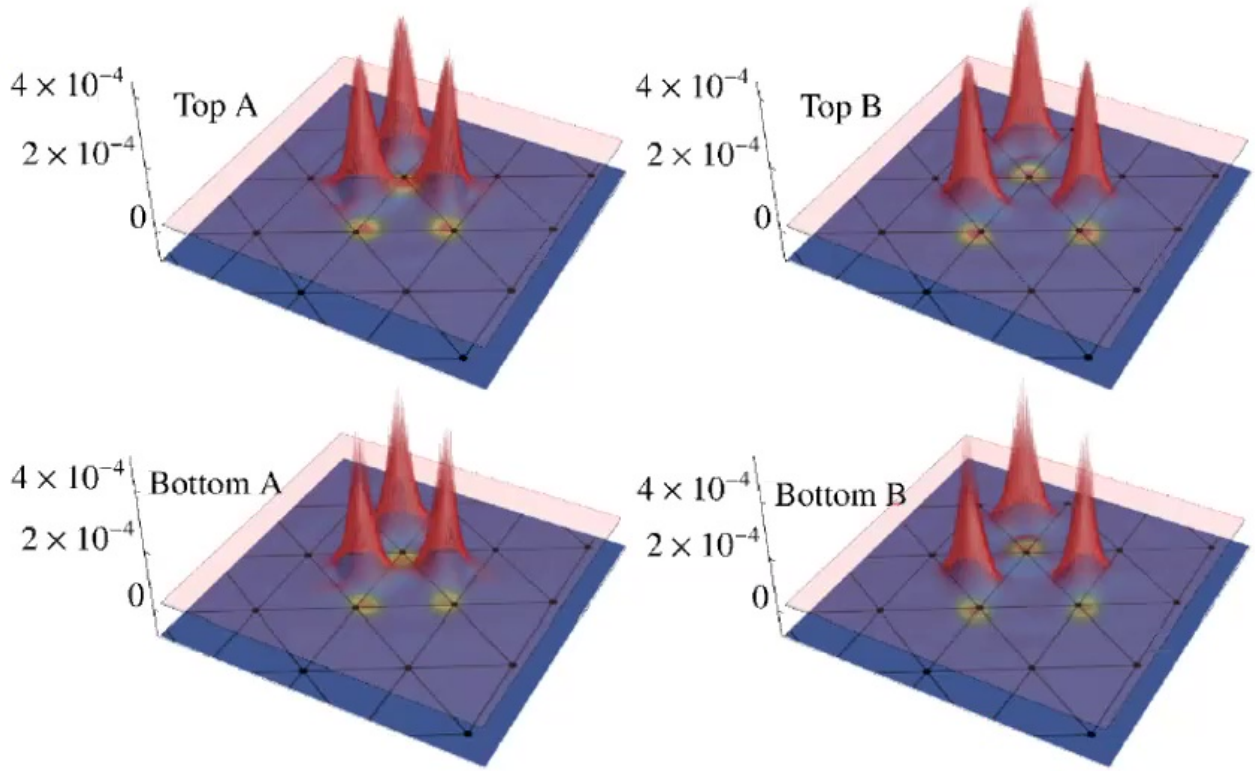

Jian Kang and OV PRX, 8, 031088 (2018)

$(m, n) = (25,26) \qquad (\theta \approx 1.3^o)$

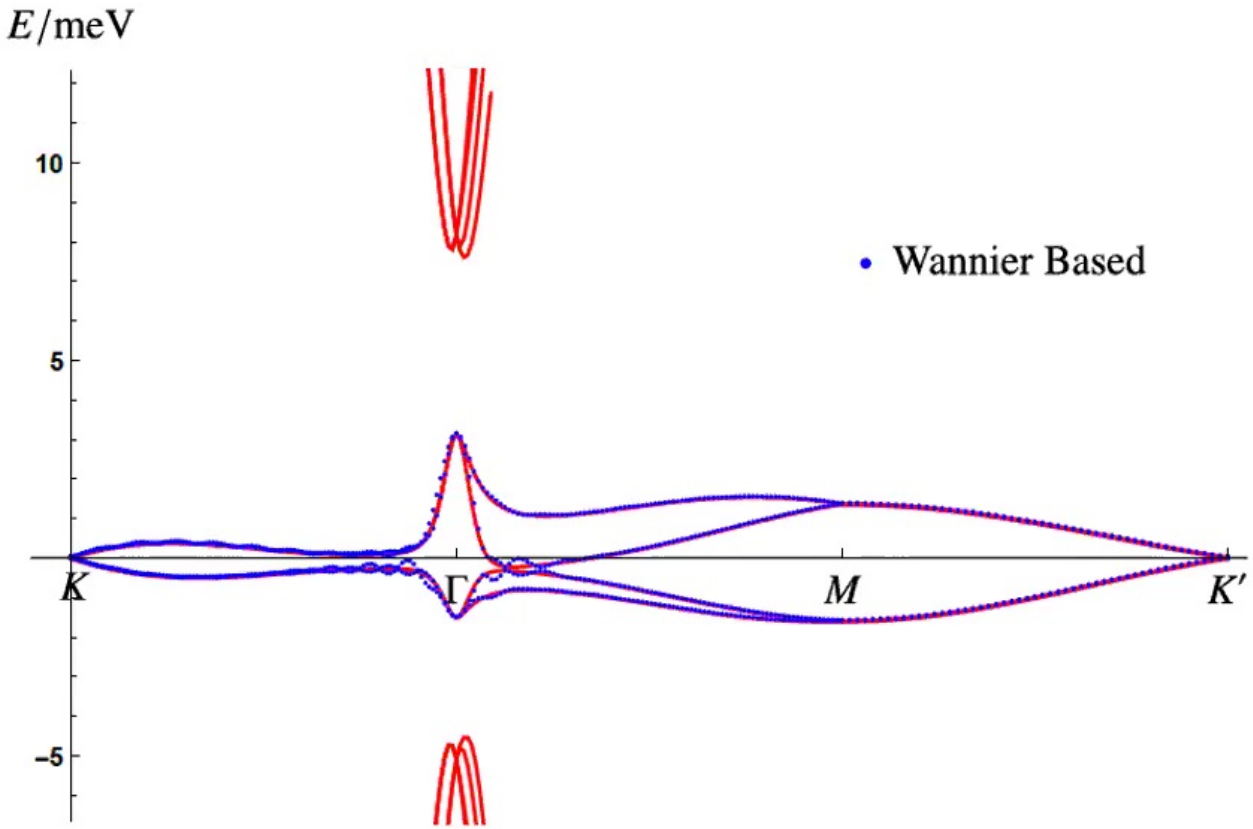

Understanding ``obstruction'' within the Wannier basis

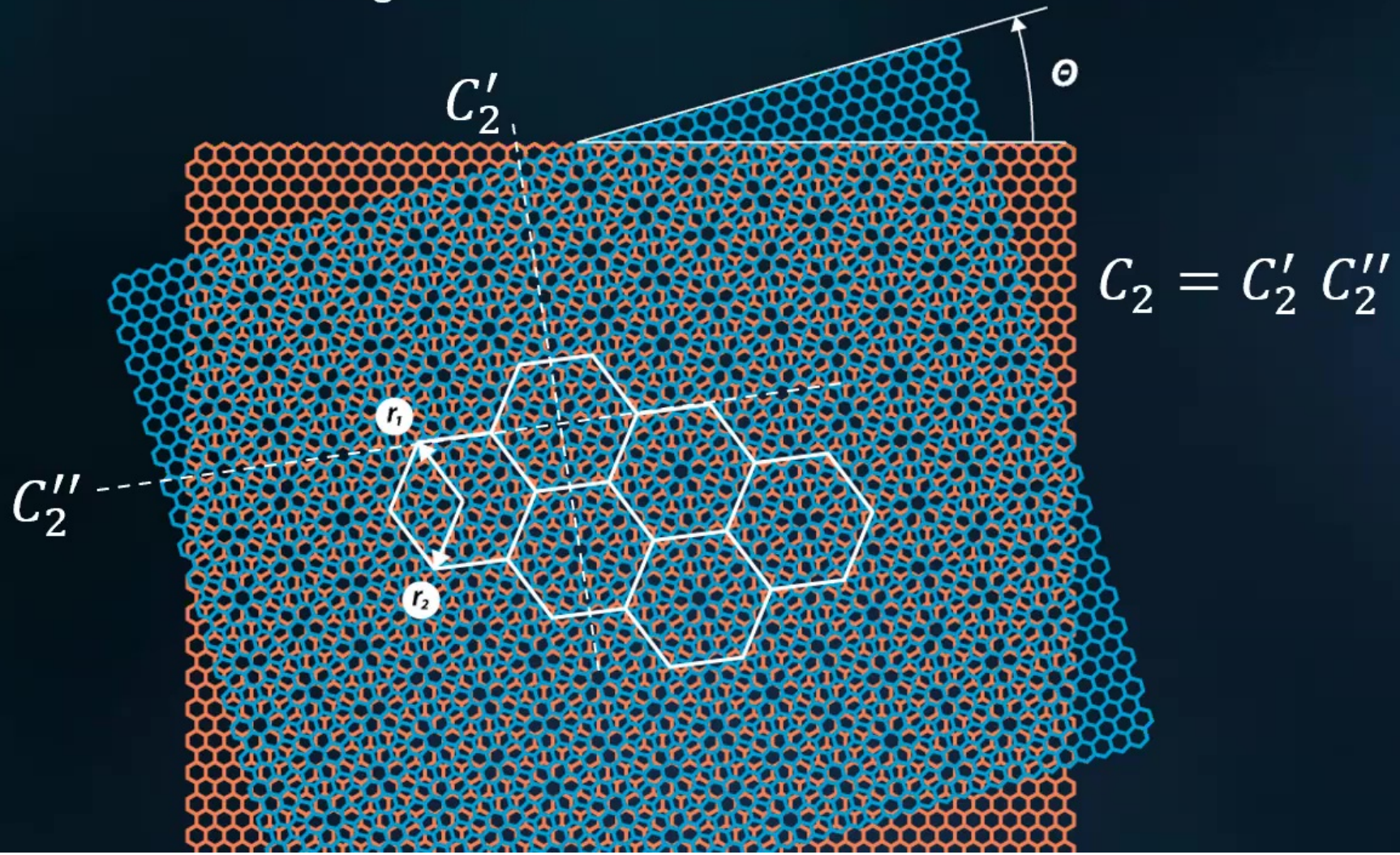

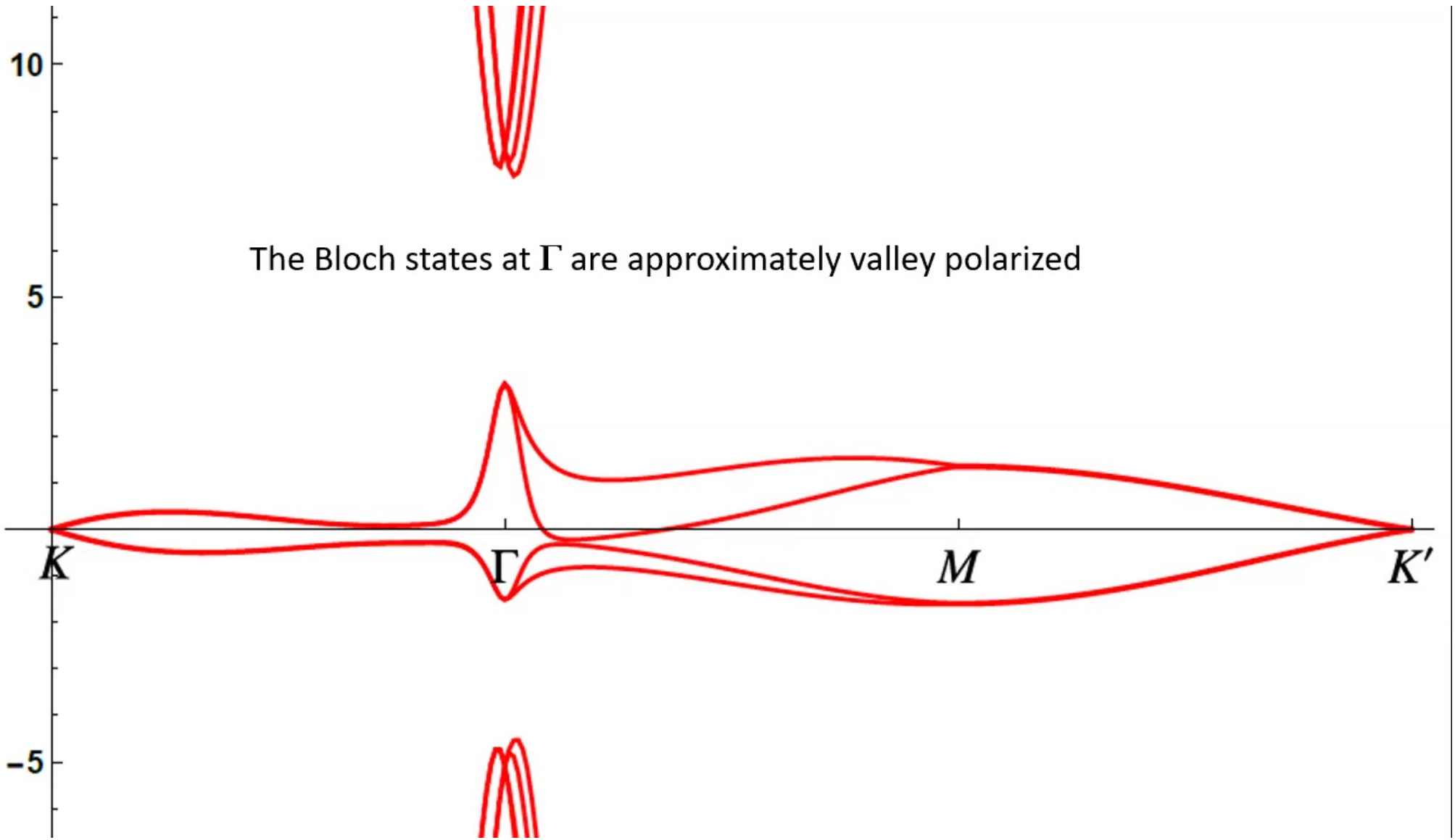

The Bloch states at Γ are approximately valley polarized

Symmetry adapted Wannier fxns

WLOG assume C_2'' even

C_2'' even

$$w_1$$
$$w_2 = w_1^*$$
$$w_3 = C_2' w_1$$
$$w_4 = w_3^*$$

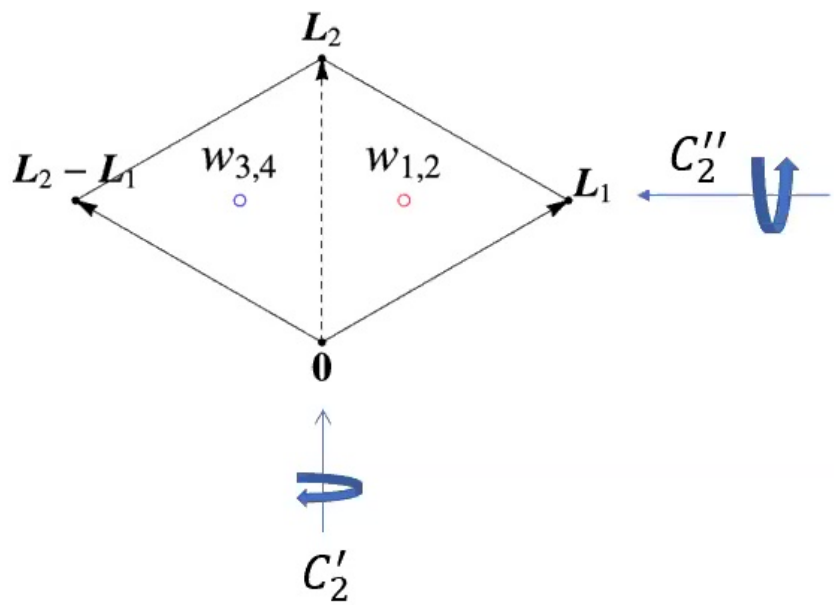

Symmetry adapted Wannier fxns

WLOG assume C_2'' even

$$w_1$$

$$w_2 = w_1^*$$

C_2'' even

$$w_3 = C_2' w_1$$

$$w_4 = w_3^*$$

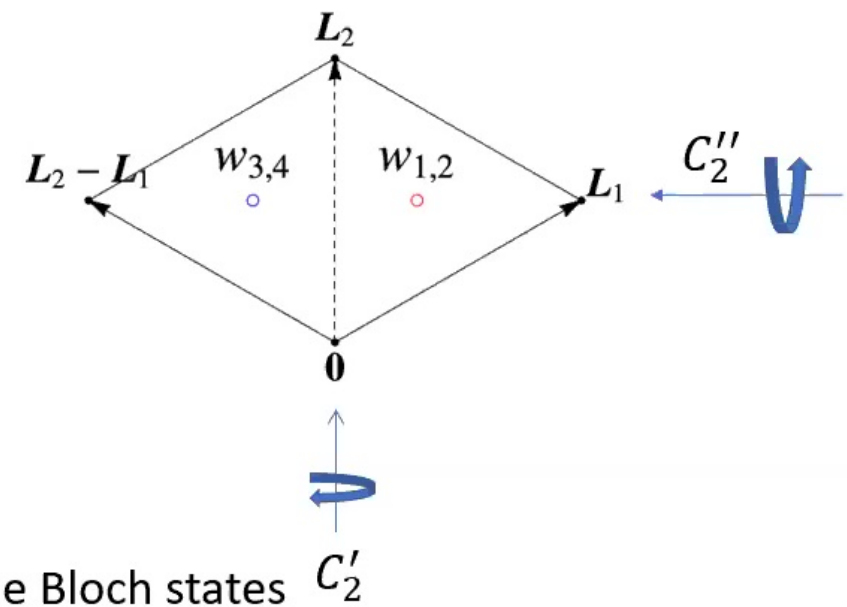

⇒ There is no way to get opposite C_2'' parity for the Bloch states

⇒ Obstruction, to implementing the emergent C_2T and $U_v(1)$ as onsite symmetries

Band topology via symmetric Wannier ``obstruction''

C_2T and $U_v(1)$ and translation

prevent construction of exponentially localized ***symmetric*** Wannier functions

symmetric: represent the crystalline, time reversal, and valley symmetries ``on-site''

H.C. Po *et al.* PRX 8, 031089 (2018); L. Zou *et al.* PRB 98, 085435 (2018)

Effective continuum model: all emergent symmetries are exact

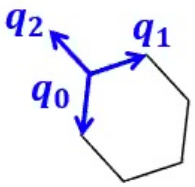

$$H_K = \int d\boldsymbol{r} \left(\psi^\dagger_{\mathcal{R}_\theta K,b}, \psi^\dagger_{K,t}\right) \begin{pmatrix} \hbar v_F \boldsymbol{p}\cdot\sigma_\theta & T(\boldsymbol{r}) \\ T^\dagger(\boldsymbol{r}) & \hbar v_F \boldsymbol{p}\cdot\sigma \end{pmatrix} \begin{pmatrix} \psi_{\mathcal{R}_\theta K,b} \\ \psi_{K,t} \end{pmatrix}$$

AA region interlayer tunneling

$$T(\boldsymbol{r}) = \begin{pmatrix} w_0 \sum_{j=0}^{2} e^{-i\boldsymbol{q}_j\cdot\boldsymbol{r}} & w_1\left(e^{-i\boldsymbol{q}_0\cdot\boldsymbol{r}} + e^{-i\phi} e^{-i\boldsymbol{q}_1\cdot\boldsymbol{r}} + e^{i\phi} e^{-i\boldsymbol{q}_2\cdot\boldsymbol{r}}\right) \\ \phi \to -\phi & w_0 \sum_{j=0}^{2} e^{-i\boldsymbol{q}_j\cdot\boldsymbol{r}} \end{pmatrix}$$

$\phi = 2\pi/3$

Bistritzer&MacDonald PNAS (2011)

Correlated electron physics in the narrow bands: RG perspective

Projecting the Coulomb interaction onto the narrow band basis should be thought of as a shortcut to integrating out the remote bands in the presence of the Coulomb interaction and determining the residual interaction within the narrow bands.

Stage 1 flow eqs:

$$\frac{dv_F}{dE_c} = -\frac{e^2}{4\epsilon}$$

$$\frac{dw_0}{dE_c} = 0$$

$$\frac{dw_1}{dE_c} = -w_1\frac{e^2}{4\epsilon}$$

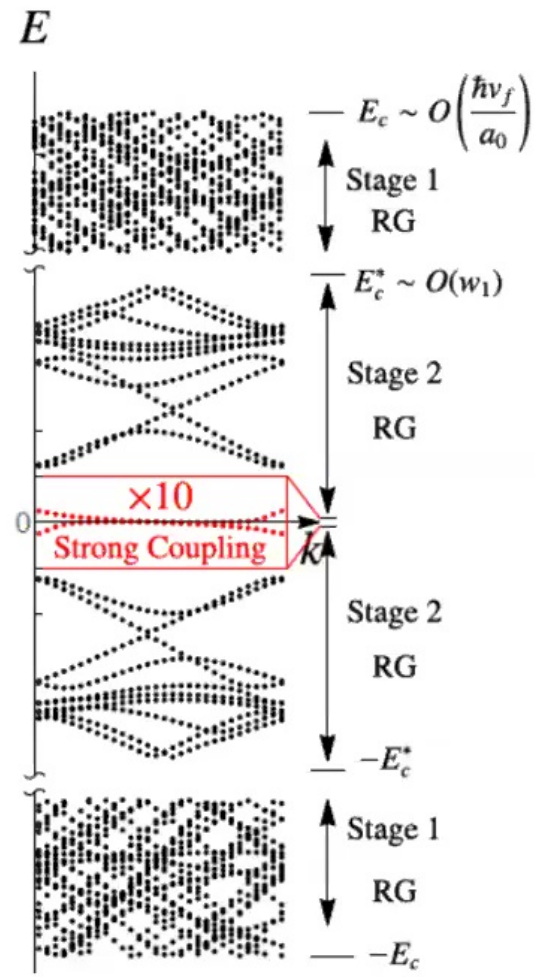

OV and J. Kang PRL2020

Advance to the next animation or slide

Correlated electron physics in the narrow bands: RG perspective

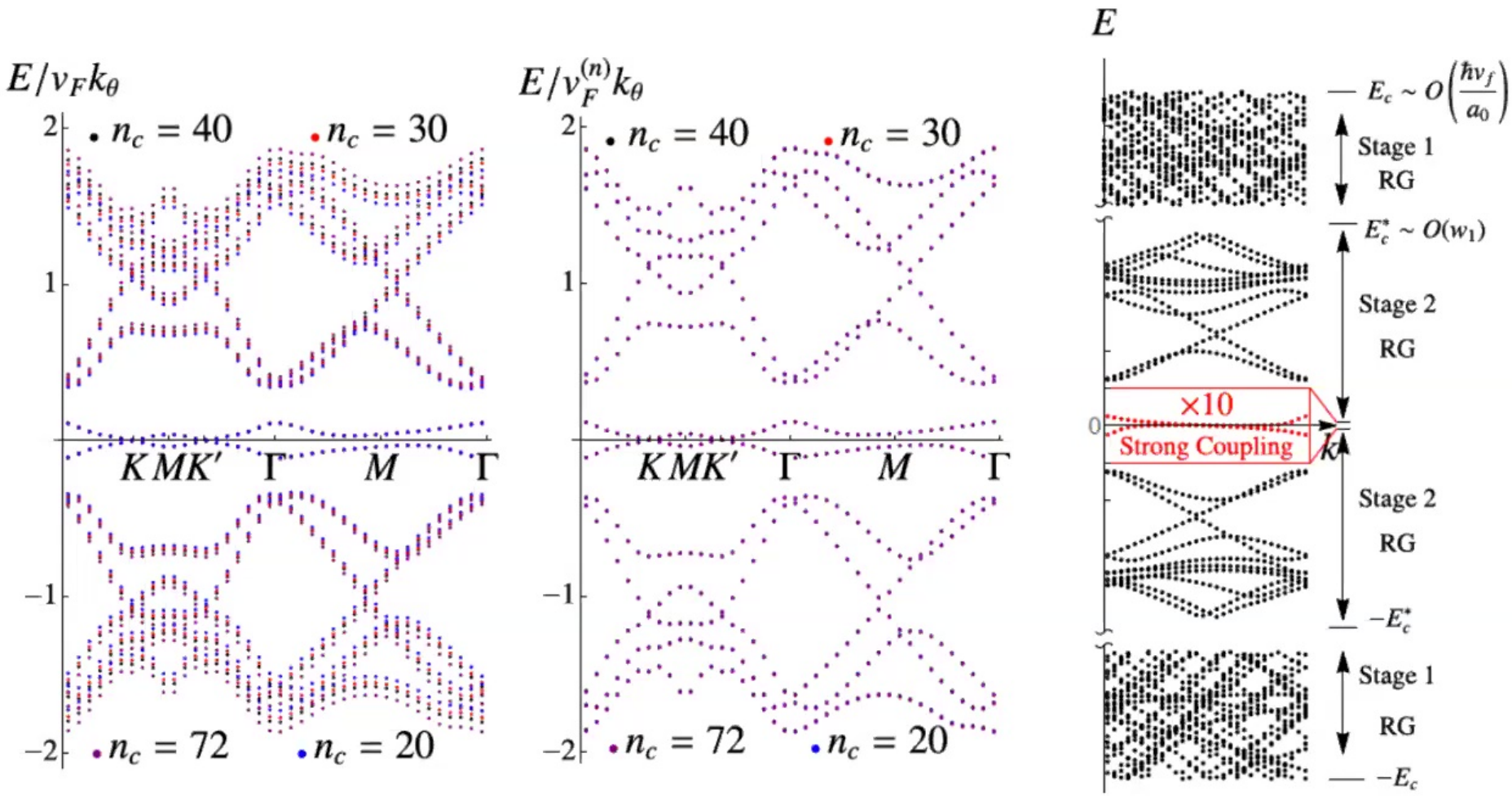

OV and J. Kang PRL2020

Gate-screened Coulomb interaction case

Image charges induced by two gates

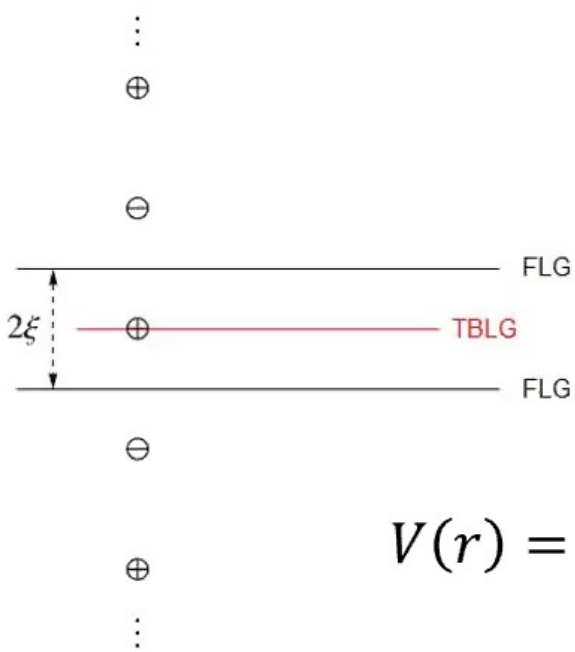

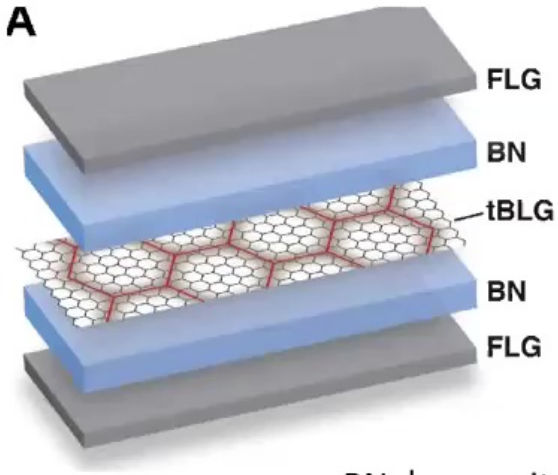

BN: boron nitride
FLG: few layer graphite

$$V(r) = \frac{e^2}{4\pi\epsilon} \sum_{n=\infty}^{\infty} \frac{(-1)^n}{\sqrt{r^2 + n^2\xi^2}}$$

Strong coupling approach: (false) expectations

$$H_{eff} = -\frac{K^2}{U} + \cdots$$

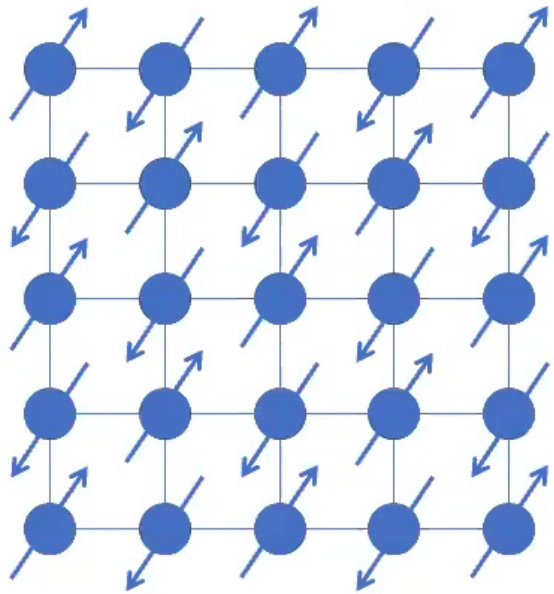

This is NOT what happens in the strong coupling limit for magic angle twisted BLG

Nonlocal Interactions

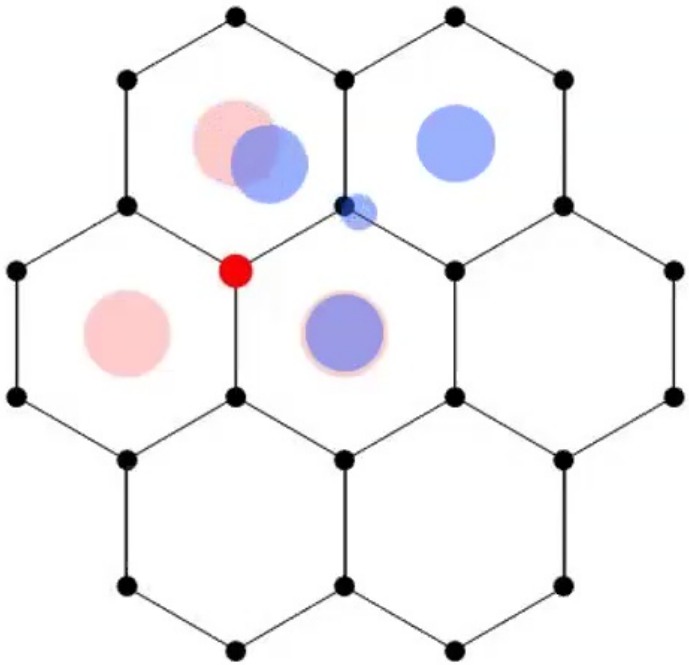

three-peak structure of WS leads to interactions beyond the Hubbard model

J. Kang and OV, PRL **122**, 246401 (2019)

Interaction form

$$V = \frac{U_0}{2} \sum_{\boldsymbol{R}} \hat{O}^2_{\boldsymbol{R}}$$

$$\hat{O}_R = \frac{1}{3}\left(\hat{N}_{\boldsymbol{R}} + \alpha_1 \hat{T}_{\boldsymbol{R}}\right)$$

$$\hat{N}_{\boldsymbol{R}} = \sum_{\tau=K,K'} \sum_{i=1}^{6} d^\dagger_{\boldsymbol{R}+\boldsymbol{\delta}_i,\tau,\sigma} d_{\boldsymbol{R}+\boldsymbol{\delta}_i,\tau,\sigma}$$

$$\hat{T}_{\boldsymbol{R}} = \sum_{i=1}^{6} \sum_{\tau=K,K'} (-1)^i d^\dagger_{\boldsymbol{R}+\boldsymbol{\delta}_i,\tau,\sigma} d_{\boldsymbol{R}+\boldsymbol{\delta}_{i+1},\tau,\sigma} + h.c.$$

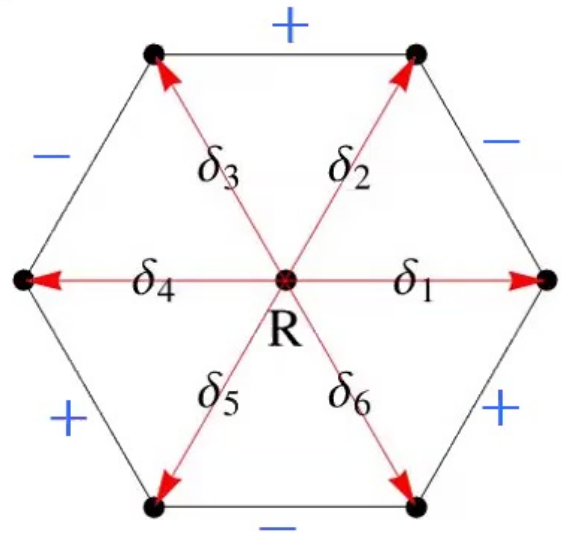

- Note that $[O_R, O_{R'}] \neq 0$ for n.n. R, R'
- the interaction induces correlations among the sites
- $\alpha_1 \sim \mathcal{O}(1)$ is a consequence of obstructed C_2'' symmetry

SU(4) FM and intervalley coherent state at *even* number of particles/holes per moire u.c.

Valley polarized state
(a ground state of projected Coulomb interaction)

Intervalley coherent state
(ground state of projected Coulomb interaction and favored by the super-exchange)

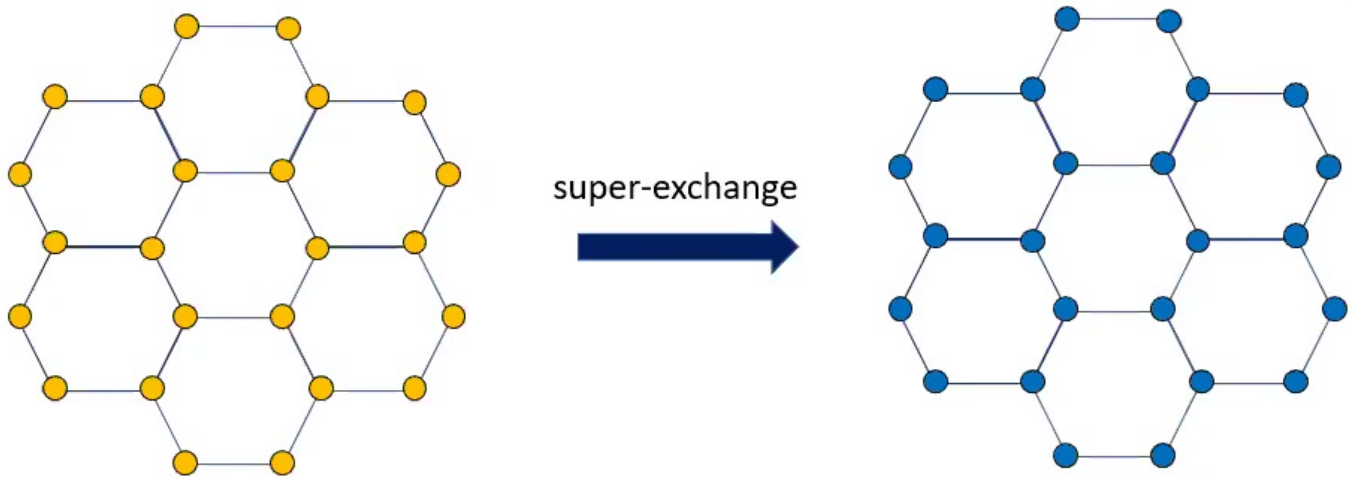

$= |K\uparrow\rangle$

$= \frac{1}{\sqrt{2}}(|K\uparrow\rangle + |K'\downarrow\rangle)$

J. Kang and OV, PRL **122**, 246401 (2019) (see also Bultinck et al PRX 2020, Bernevig et al 2020 TBG series for more on IVCs with different symmetries).

SU(4) FM and odd number particles/holes per moire u.c.

(assuming spin and valley polarized)

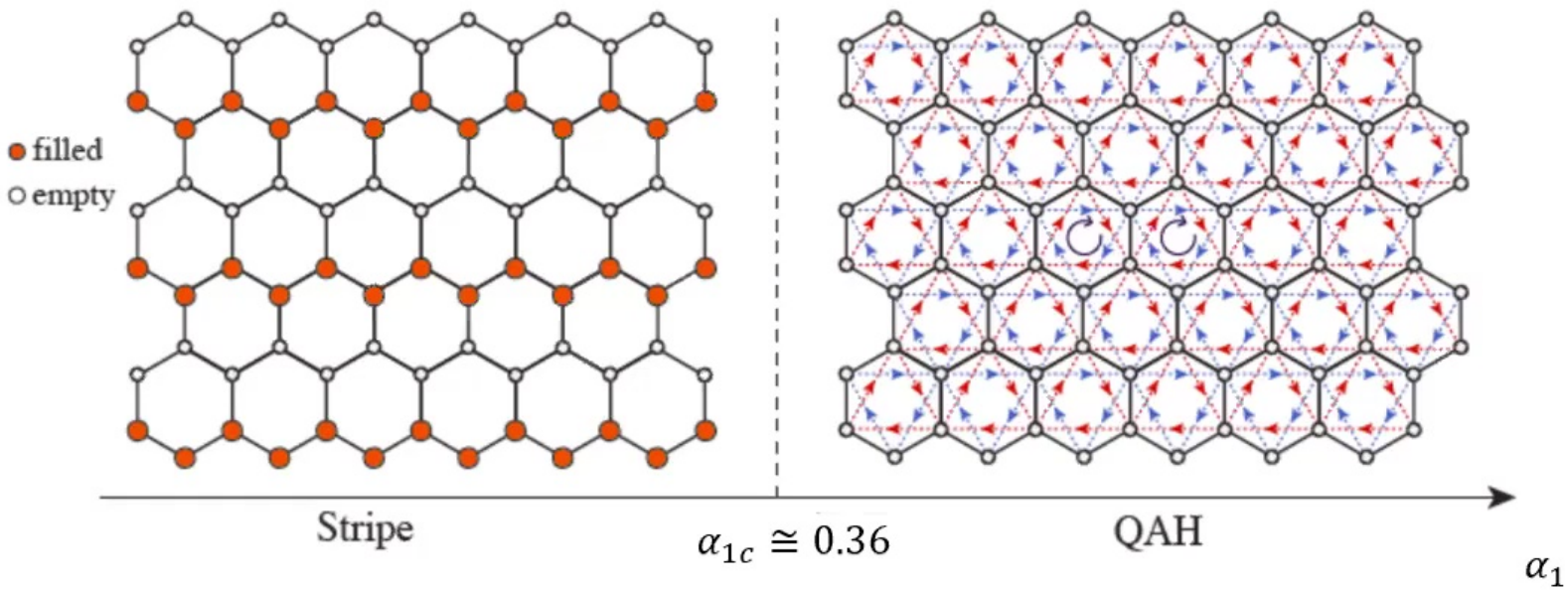

J. Kang and OV, PRL **122**, 246401 (2019)

Bin-Bin Chen, Yuan Da Liao, Ziyu Chen, OV, Jian Kang, Wei Li, Zi Yang Meng arXiv:2011.07602

(see also Jian Kang and Oskar Vafek, PRB 102, 035161 (2020))

2D exponentially localized Wannier states

Advantages:

- Interactions are straightforward
- Generalized ferromagnetism and some of the insulating phases can be intuitively understood

Disadvantages:

- C_2T and C_2'' are encoded non-locally and additional work is needed to determine whether a many body state respects or breaks them

Hybrid Wannier basis: motivation

- Exponentially localized WSs allowed us to obtain an understanding of the real space interaction and to identify the generalized **spin-valley ferromagnetism** as the dominant ordering tendency in the strong coupling limit. This tendency is due to the topologically non-trivial bands.
- In order to gain a clearer understanding of the effects of the Coulomb interaction on the $U_v(1)$ and C_2T symmetries of the low energy states, we now use (hybrid) Wannier basis which is localized only in one direction and are extended Bloch waves in the other direction. Additional advantages of this basis are that the topology of the narrow bands is more transparent and that states with broken translational symmetry in the localized direction can be readily described. The disadvantage is the complicated form the Coulomb interaction takes in the hybrid Wannier basis making its effect less transparent.

Effective continuum model: all emergent symmetries are exact

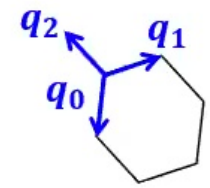

$$H_K = \int d\boldsymbol{r} \left(\psi^\dagger_{\mathcal{R}_\theta K,b}, \psi^\dagger_{K,t}\right) \begin{pmatrix} \hbar v_F \boldsymbol{p}\cdot\sigma_\theta & T(\boldsymbol{r}) \\ T^\dagger(\boldsymbol{r}) & \hbar v_F \boldsymbol{p}\cdot\sigma \end{pmatrix} \begin{pmatrix} \psi_{\mathcal{R}_\theta K,b} \\ \psi_{K,t} \end{pmatrix}$$

$$T(\boldsymbol{r}) = \begin{pmatrix} w_0 \sum_{j=0}^{2} e^{-i\boldsymbol{q}_j\cdot\boldsymbol{r}} & w_1\left(e^{-i\boldsymbol{q}_0\cdot\boldsymbol{r}} + e^{-i\phi} e^{-i\boldsymbol{q}_1\cdot\boldsymbol{r}} + e^{i\phi} e^{-i\boldsymbol{q}_2\cdot\boldsymbol{r}}\right) \\ \phi \to -\phi & w_0 \sum_{j=0}^{2} e^{-i\boldsymbol{q}_j\cdot\boldsymbol{r}} \end{pmatrix}$$

$\phi = 2\pi/3$

Bistritzer&MacDonald PNAS (2011)

Hybrid Wannier basis

Projected position operator along g_1: $\hat{\mathcal{P}} e^{-i\delta \boldsymbol{q}\cdot\boldsymbol{r}} \hat{\mathcal{P}}$

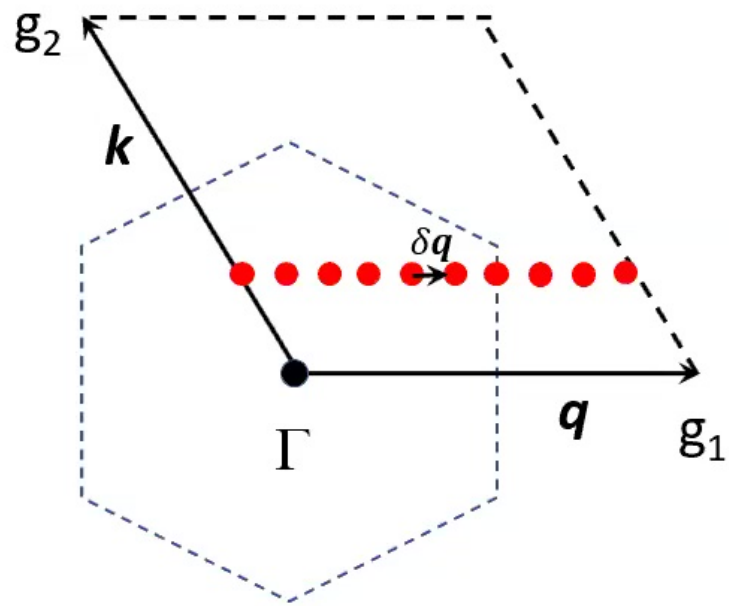

R. Yu, X. L. Qi, B. A. Bernevig, Z. Fang, and X. Dai, PRB 84, 075119 (2011)

Hybrid Wannier basis

Projected position operator along g_1: $\hat{\mathcal{P}} e^{-i\delta \boldsymbol{q}\cdot \boldsymbol{r}} \hat{\mathcal{P}}$

seek eigenstates of the form: $\sum_b \sum_{j=0}^{N-1} \alpha_{j,b} \, |\boldsymbol{k} + j\, \delta \boldsymbol{q}, b\rangle$

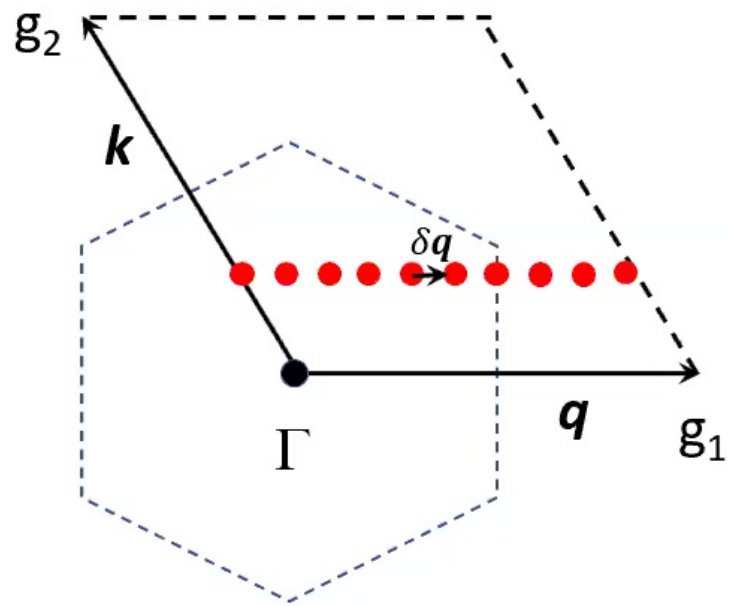

Then, $\Lambda_{bb'}(\boldsymbol{k}, j)\, \alpha_{j+1,b} = \epsilon_{\boldsymbol{k}} \alpha_{j,b}$ where

$$\Lambda_{bb'}(\boldsymbol{k}, j) = \langle u_{\boldsymbol{k}+j\,\delta \boldsymbol{q},b} | u_{\boldsymbol{k}+(j+1)\,\delta \boldsymbol{q},b'} \rangle$$

$$\Lambda(\boldsymbol{k}, 0)\Lambda(\boldsymbol{k}, 1)\ldots\Lambda(\boldsymbol{k}, \mathrm{N}-1)\alpha_0 = \epsilon_{\boldsymbol{k}}^N \alpha_0$$

$$\Lambda(\boldsymbol{k}, 0)\Lambda(\boldsymbol{k}, 1)\ldots\Lambda(\boldsymbol{k}, \mathrm{N}-1) = e^{-2\pi i \langle x/L_m \rangle \sigma_2}$$

R. Yu, X. L. Qi, B. A. Bernevig, Z. Fang, and X. Dai, PRB 84, 075119 (2011)

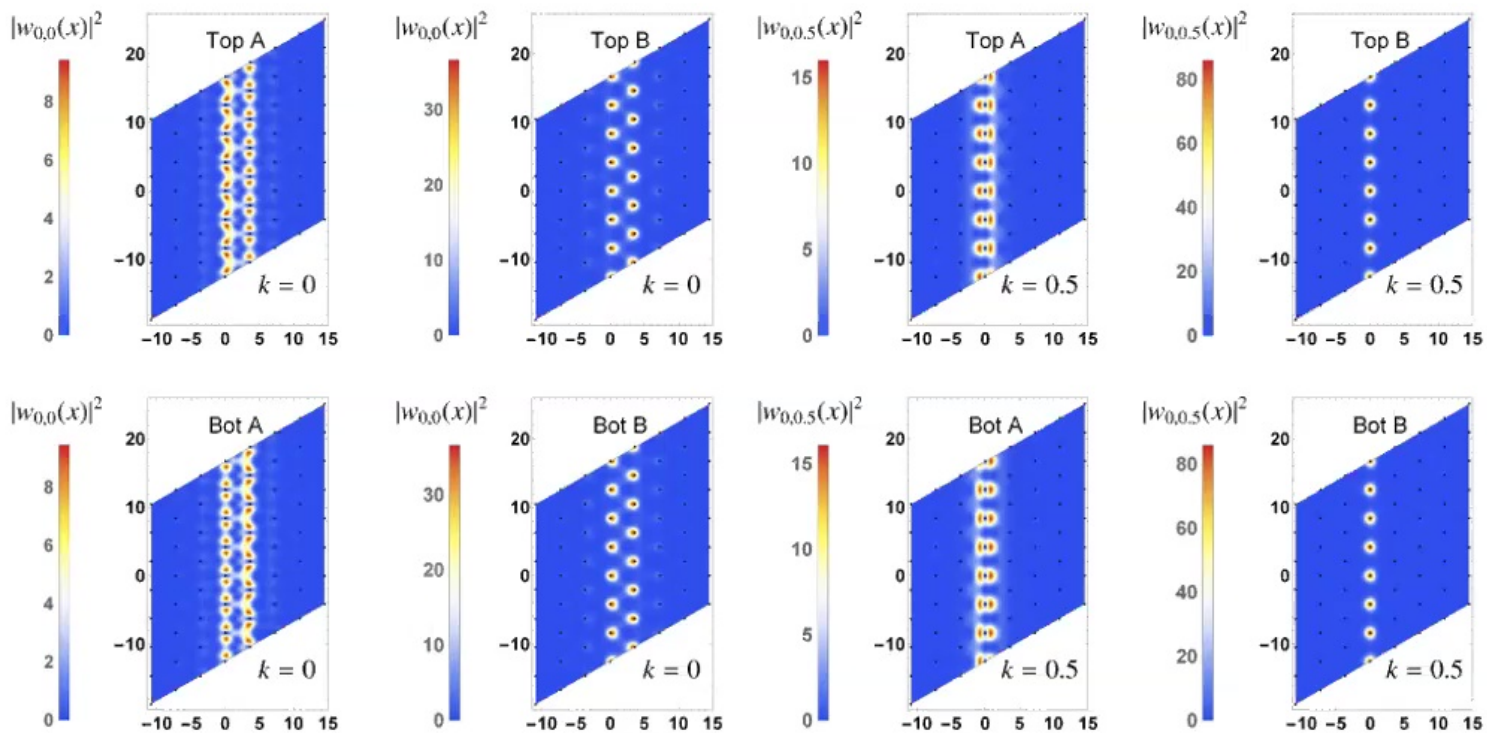

J. Kang and OV, PRB 102, 035161 (2020)

Band topology via the hybrid Wannier basis: Wilson loops

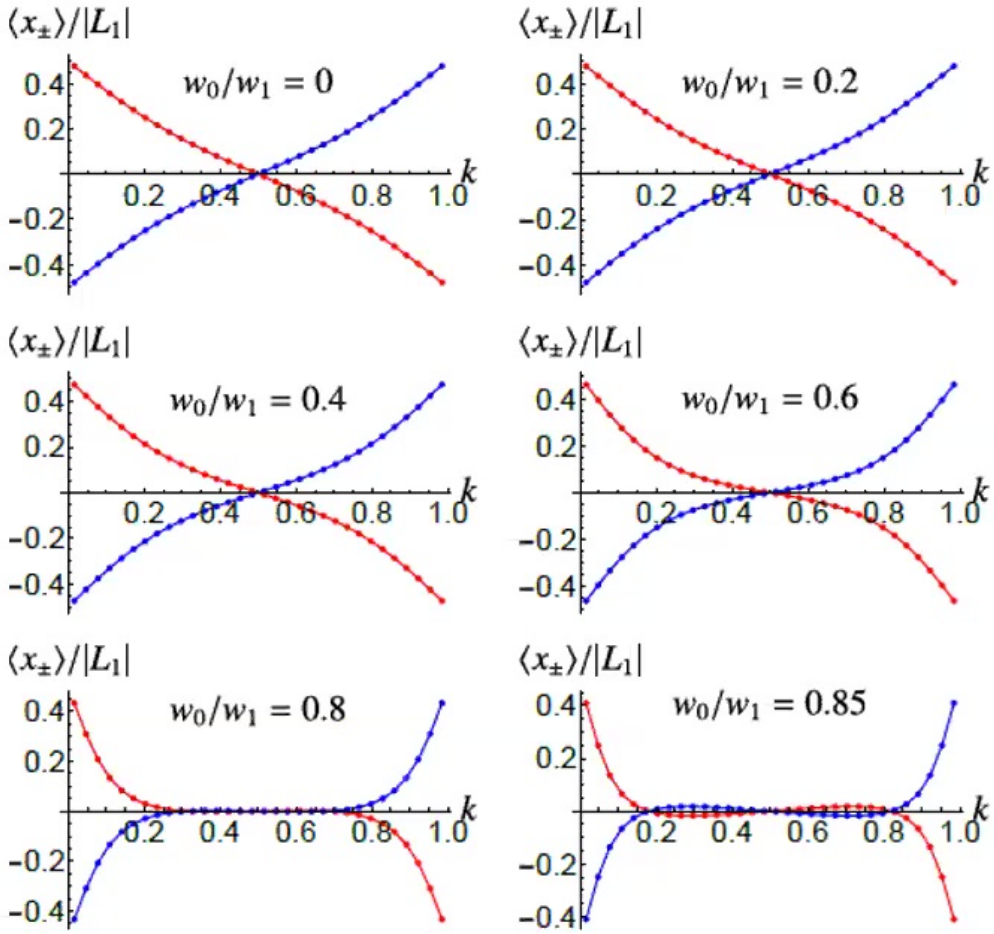

J. Kang and OV, PRB 102, 035161 (2020) (see also Bernevig et al PRL 2019)

Evolution of the Wilson loop under RG

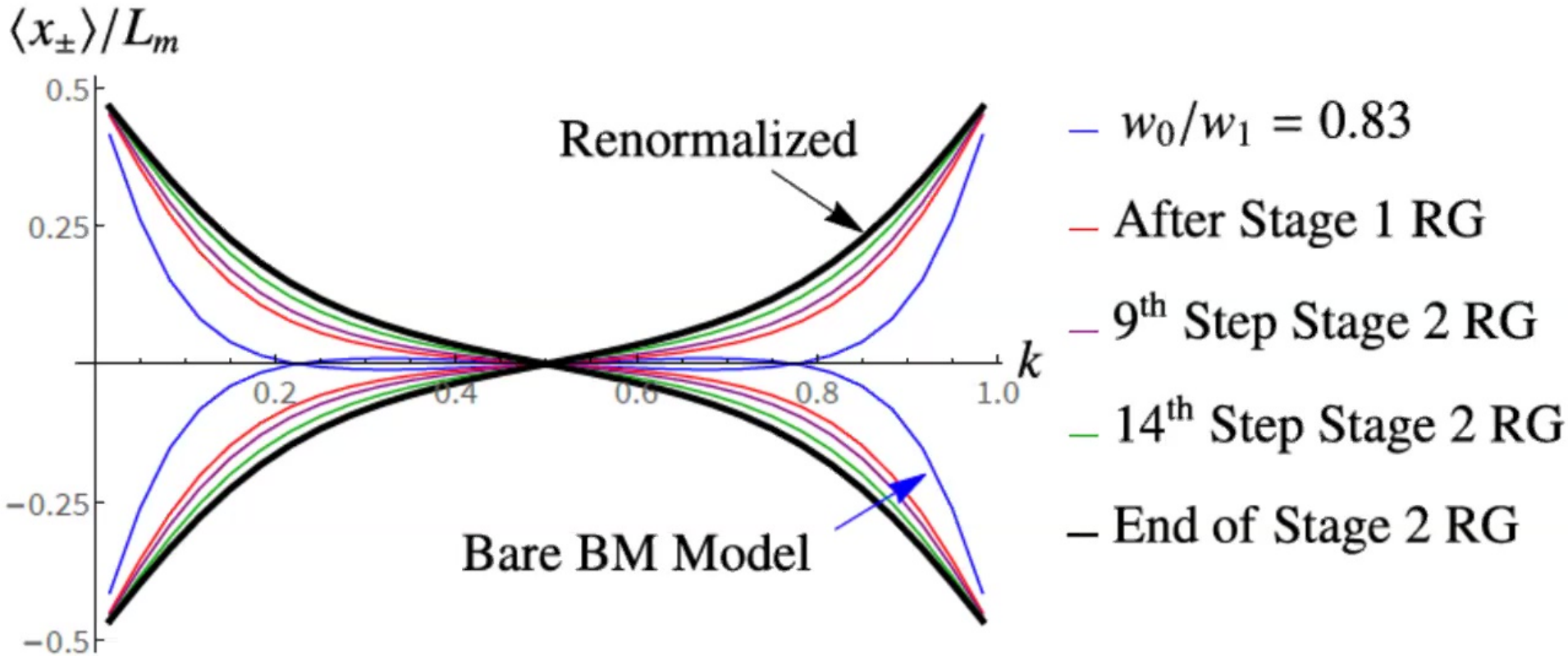

OV and Jian Kang PRL2020

Band topology via smooth gauge Chern ± 1 Bloch states

$$|\phi_{\pm}(q,k\rangle = \frac{1}{\sqrt{N}}\sum_{n} e^{2\pi i q n}\,|w_{\pm}(n,k\boldsymbol{g_2}\rangle$$

$$H_{kin} = 1_2 n_0(q,k) + \sigma_1 n_1(q,k) + \sigma_2 n_2(q,k)$$

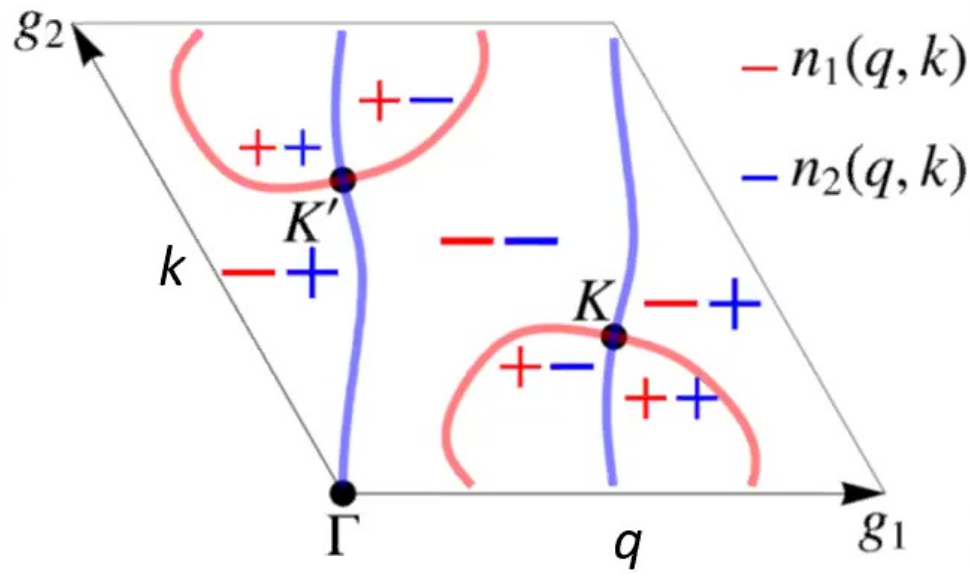

J. Kang and OV, PRB 102, 035161 (2020); See also H.C. Po *et al.* PRX(2018); L. Zou *et al.* PRB (2018)

(iTensor) DMRG results

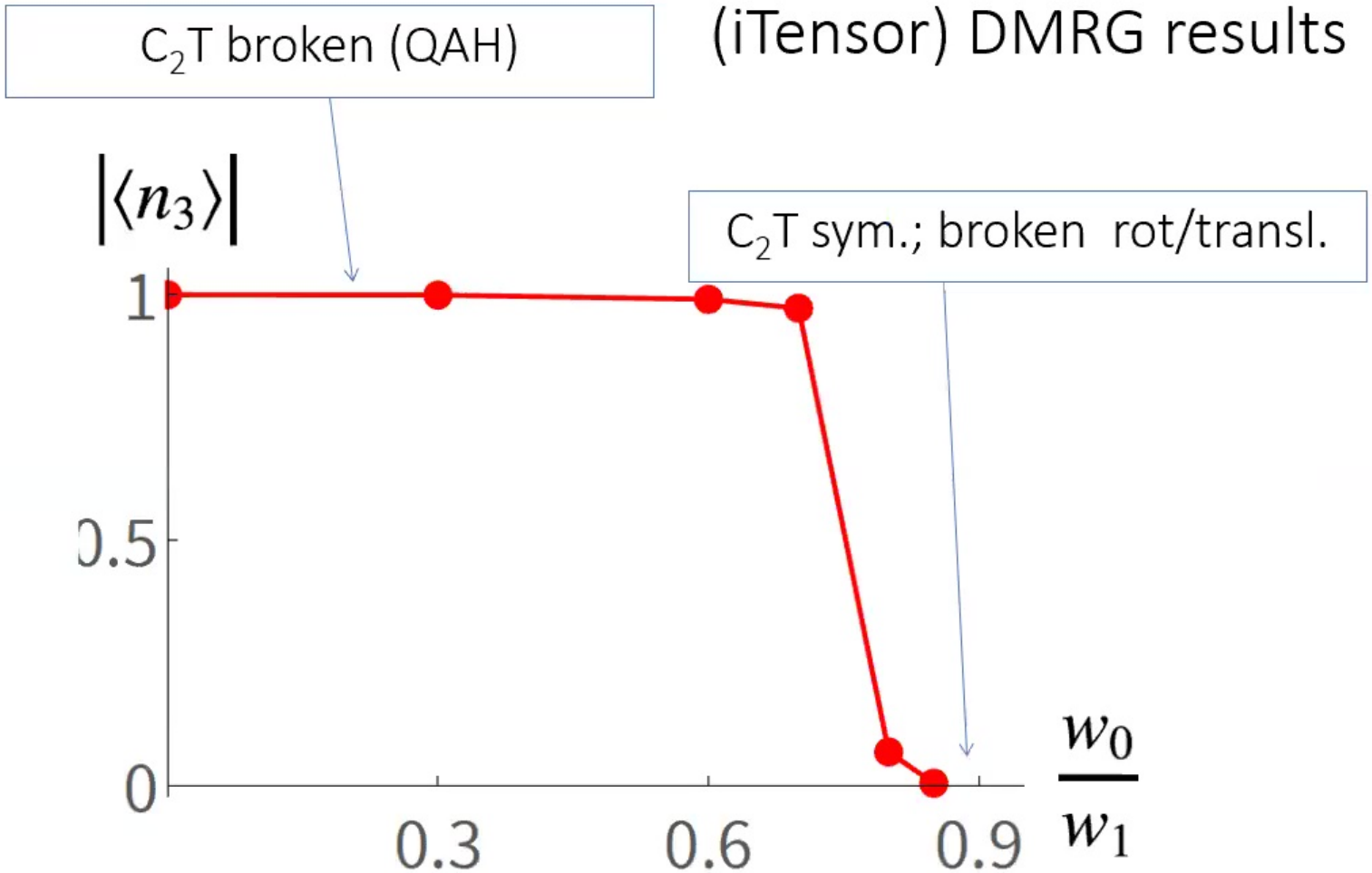

J. Kang and OV, PRB 102, 035161 (2020)

(iTensor) DMRG results: almost exclusively single occupancy

(n,k)	$(0,\frac{1}{12})$	$(0,\frac{1}{4})$	$(0,\frac{5}{12})$	$(0,\frac{7}{12})$	$(0,\frac{3}{4})$	$(0,\frac{11}{12})$
$P(\hat{N}_{n,k}=0)$	0.038	0.017	0.018	0.018	0.018	0.036
$P(\hat{N}_{n,k}=1)$	0.922	0.966	0.965	0.964	0.965	0.924
$P(\hat{N}_{n,k}=2)$	0.040	0.017	0.017	0.018	0.017	0.040

J. Kang and OV, PRB 102, 035161 (2020)

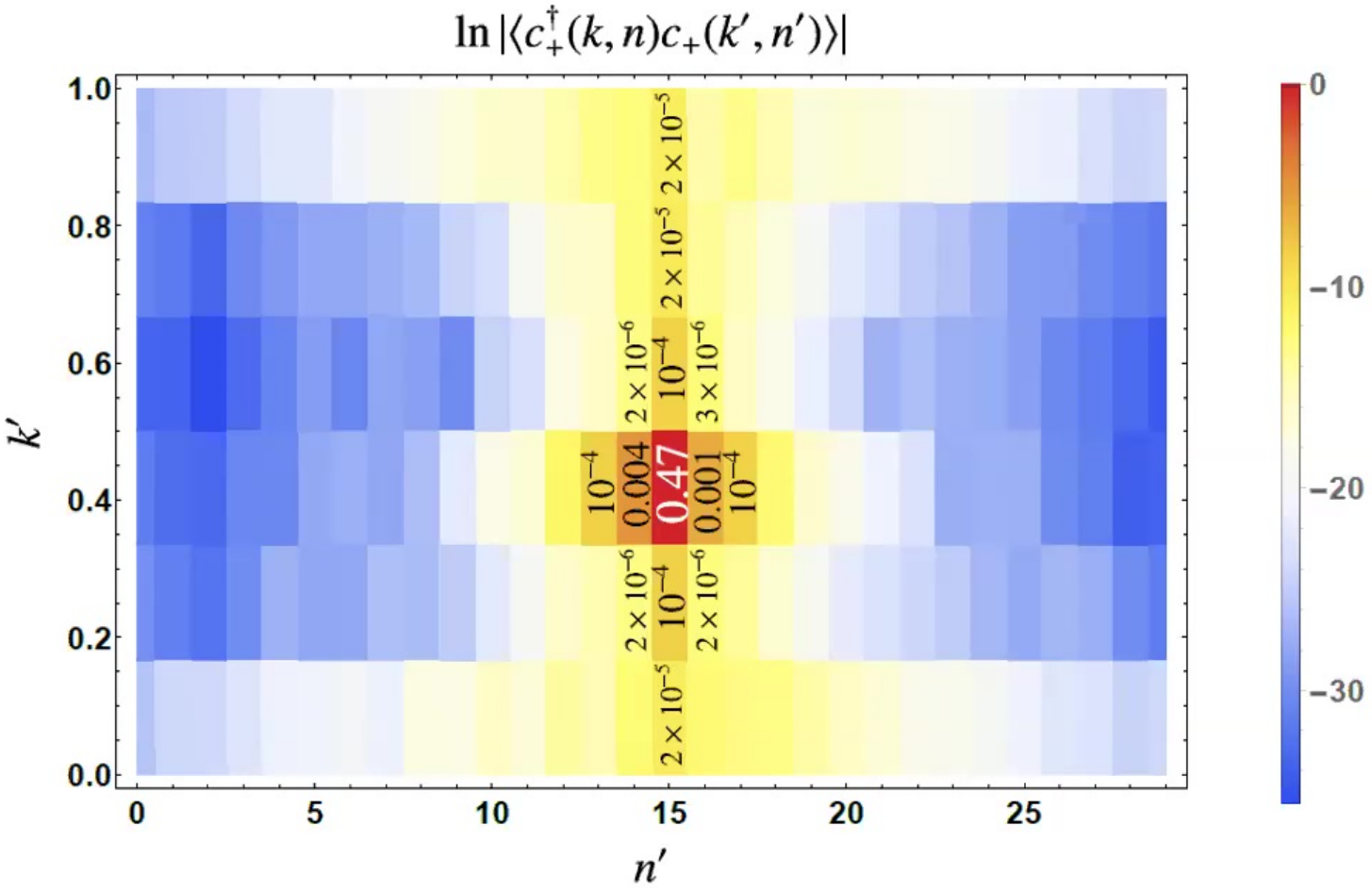

J. Kang and OV arXiv:2002.10360

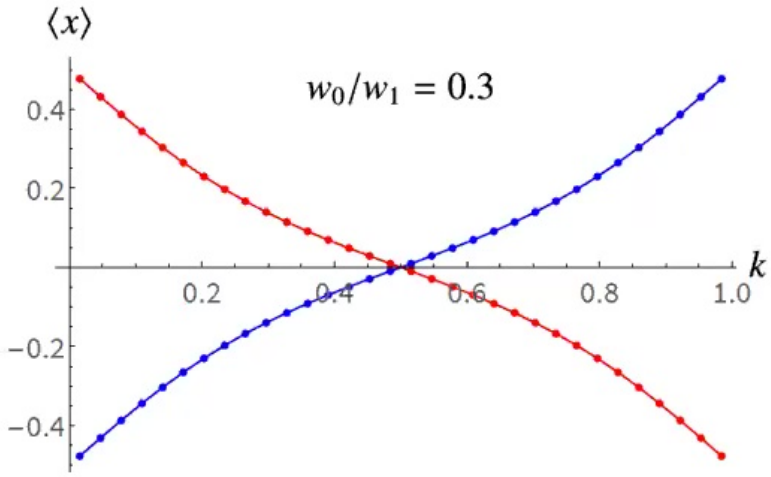
$\langle x \rangle$
$w_0/w_1 = 0.3$
0.4
0.2
−0.2
−0.4
0.2
0.4
0.6
0.8
1.0
k

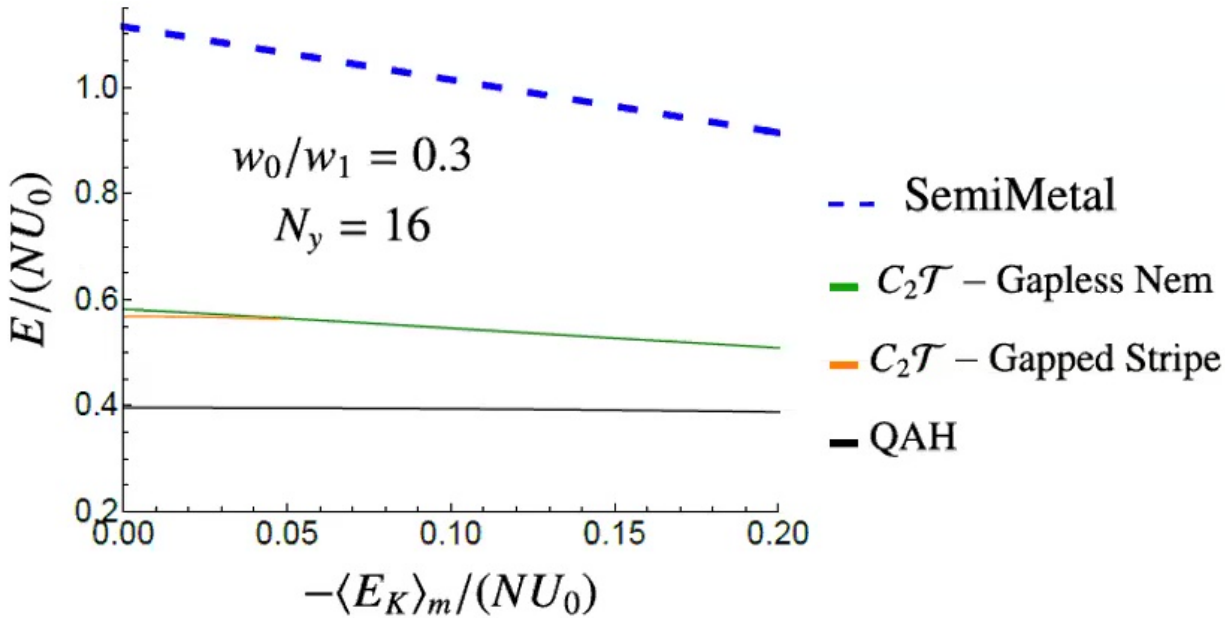
$w_0/w_1 = 0.3$
$N_y = 16$
$E/(NU_0)$
1.0
0.8
0.6
0.4
0.2
0.00
0.05
0.10
0.15
0.20
$-\langle E_K \rangle_m/(NU_0)$
SemiMetal
$C_2\mathcal{T}$ – Gapless Nem
$C_2\mathcal{T}$ – Gapped Stripe
QAH

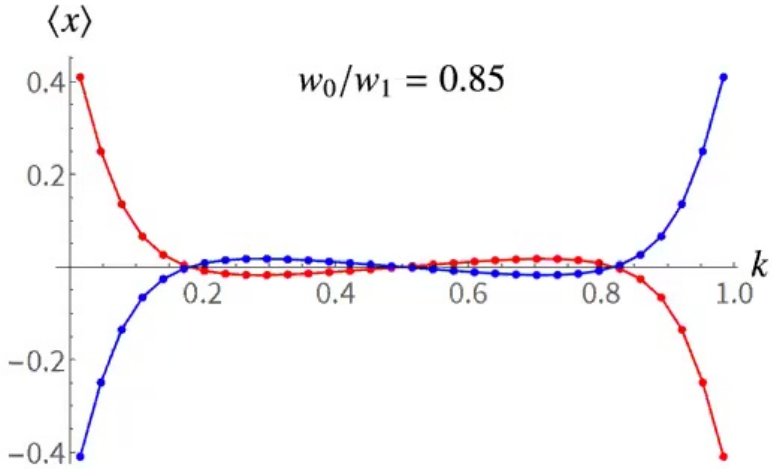
$\langle x \rangle$
$w_0/w_1 = 0.85$
0.4
0.2
−0.2
−0.4
0.2
0.4
0.6
0.8
1.0
k

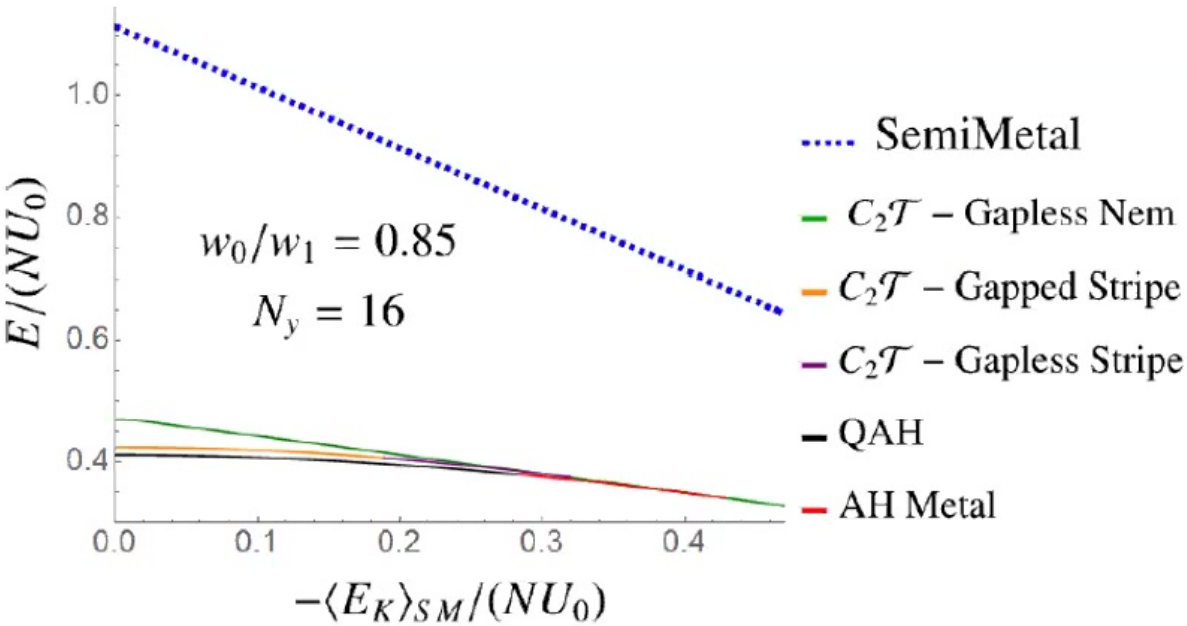
$E/(NU_0)$
1.0
0.8
0.6
0.4
$w_0/w_1 = 0.85$
$N_y = 16$
0.0
0.1
0.2
0.3
0.4
$-\langle E_K \rangle_{SM}/(NU_0)$
SemiMetal
$C_2\mathcal{T}$ – Gapless Nem
$C_2\mathcal{T}$ – Gapped Stripe
$C_2\mathcal{T}$ – Gapless Stripe
QAH
AH Metal

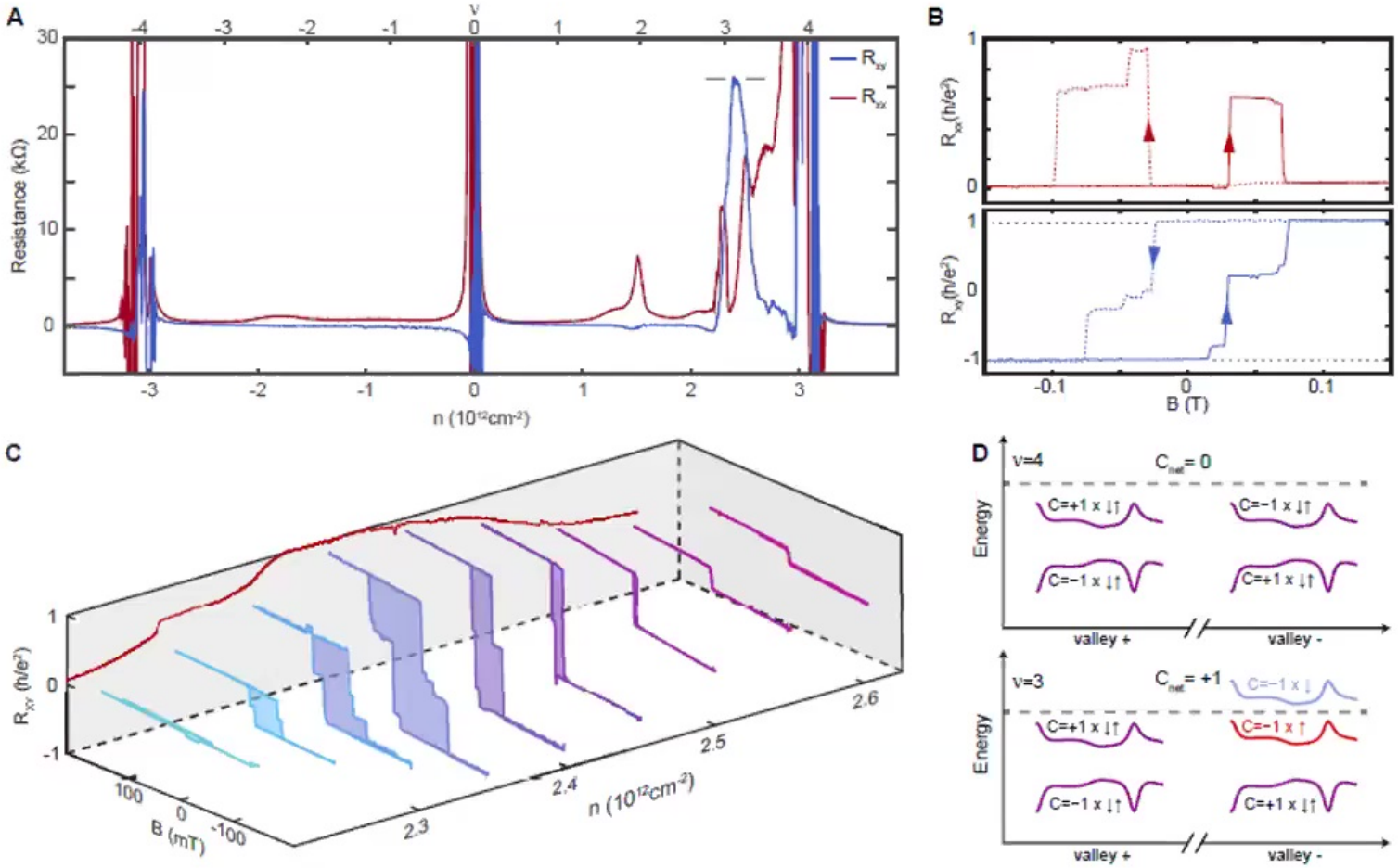

A.L. Sharpe et al Science (2019); M. Serlin et al Science (2020)

Excitation spectrum

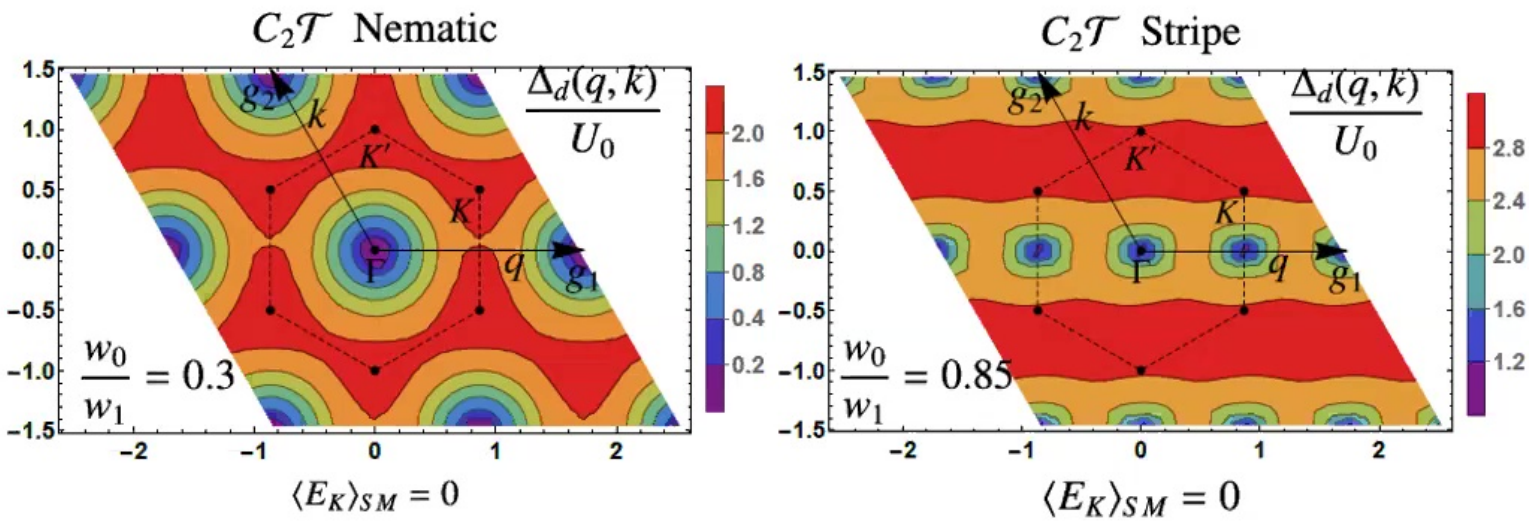

gapless

gapped

J. Kang and OV PRB 2020

Excitation spectrum

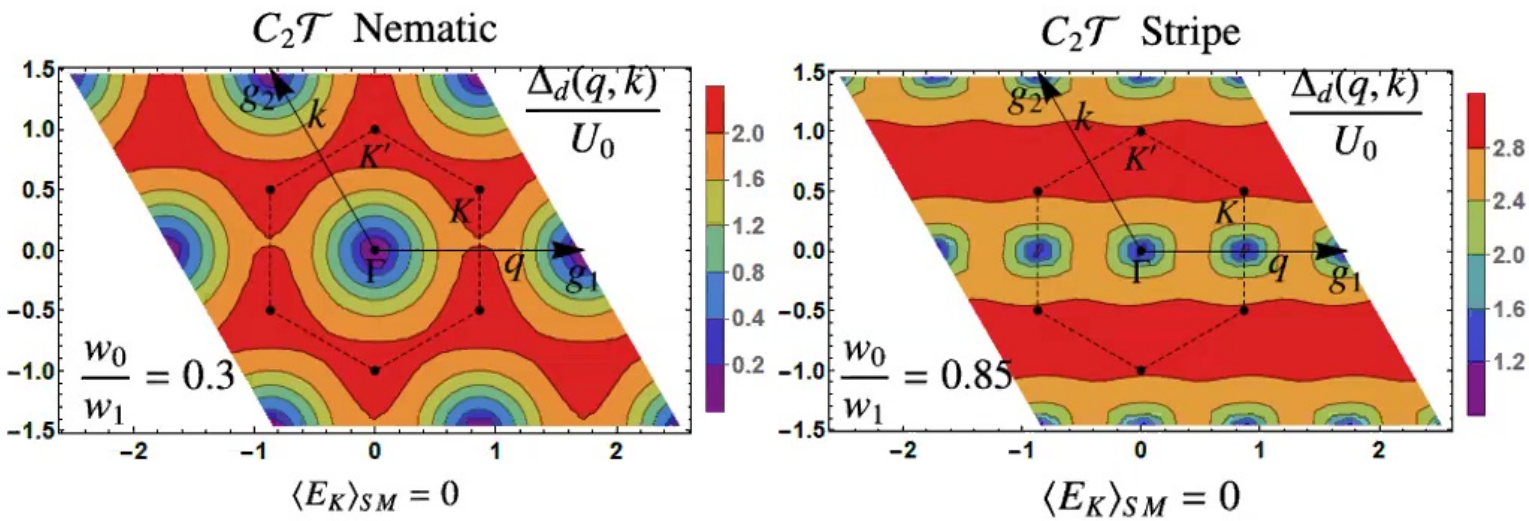

gapless

J. Kang and OV PRB 2020

Recall: equal winding number of Dirac nodes

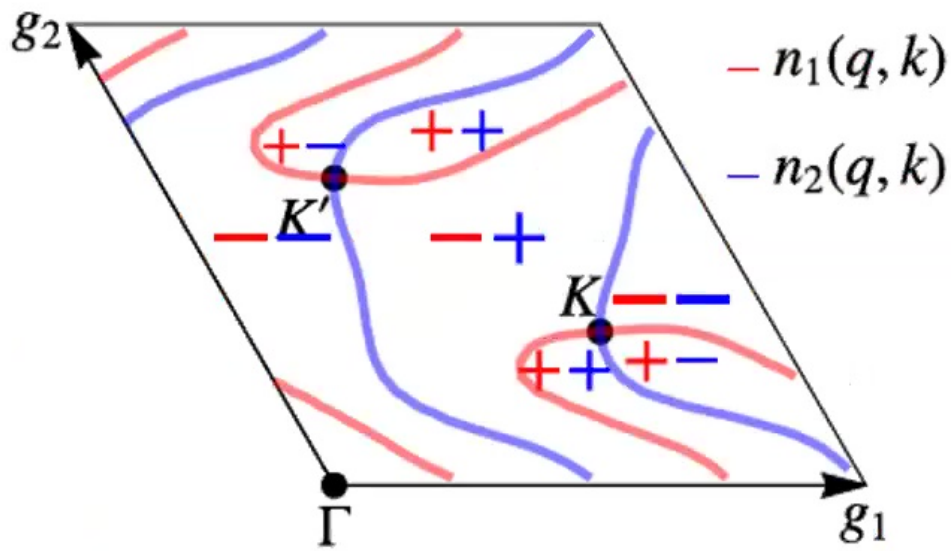

Once translational symmetry is broken, the topological charge of Dirac nodes is path dependent

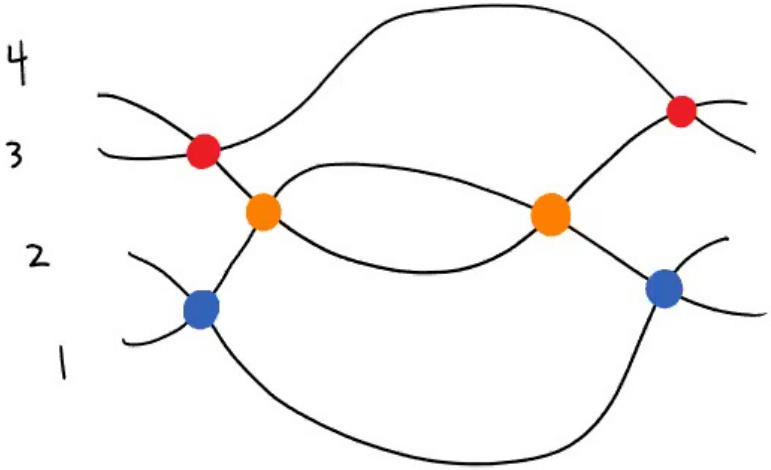

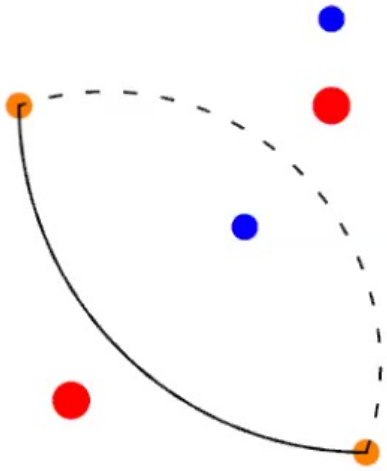

J. Kang and OV, PRB 102, 035161 (2020)
See also: Wu, Soluyanov and Bzdusek Science (2019)

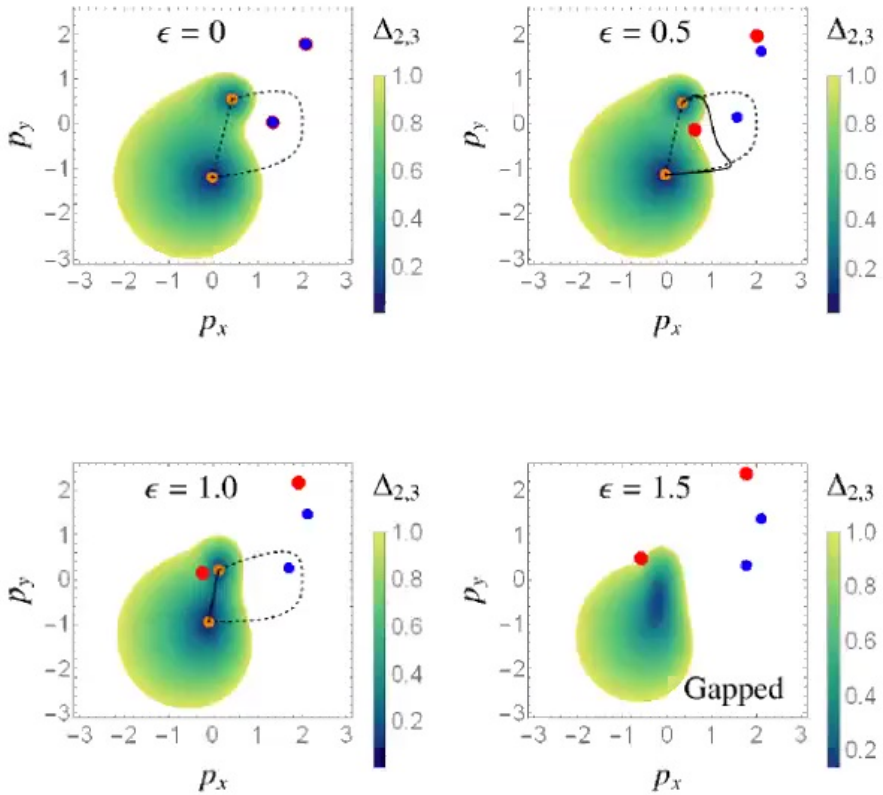

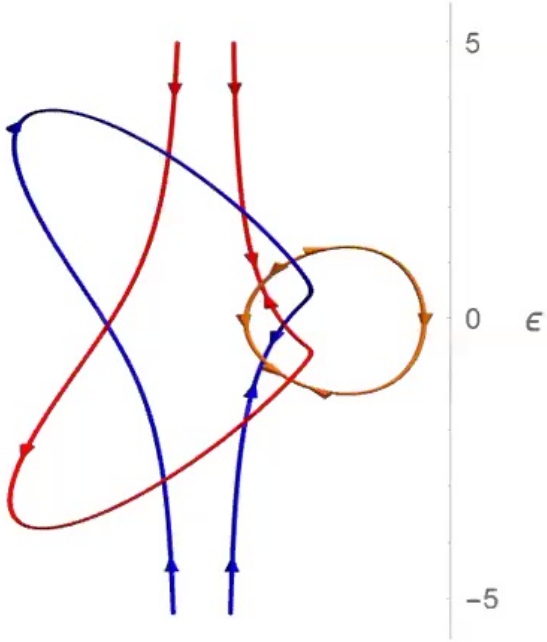

J. Kang and OV, PRB 102, 035161 (2020)
See also: Wu, Soluyanov and Bzdusek Science (2019)

Subsequently confirmed by a more accurate DMRG algorithm (Zaletel's group)

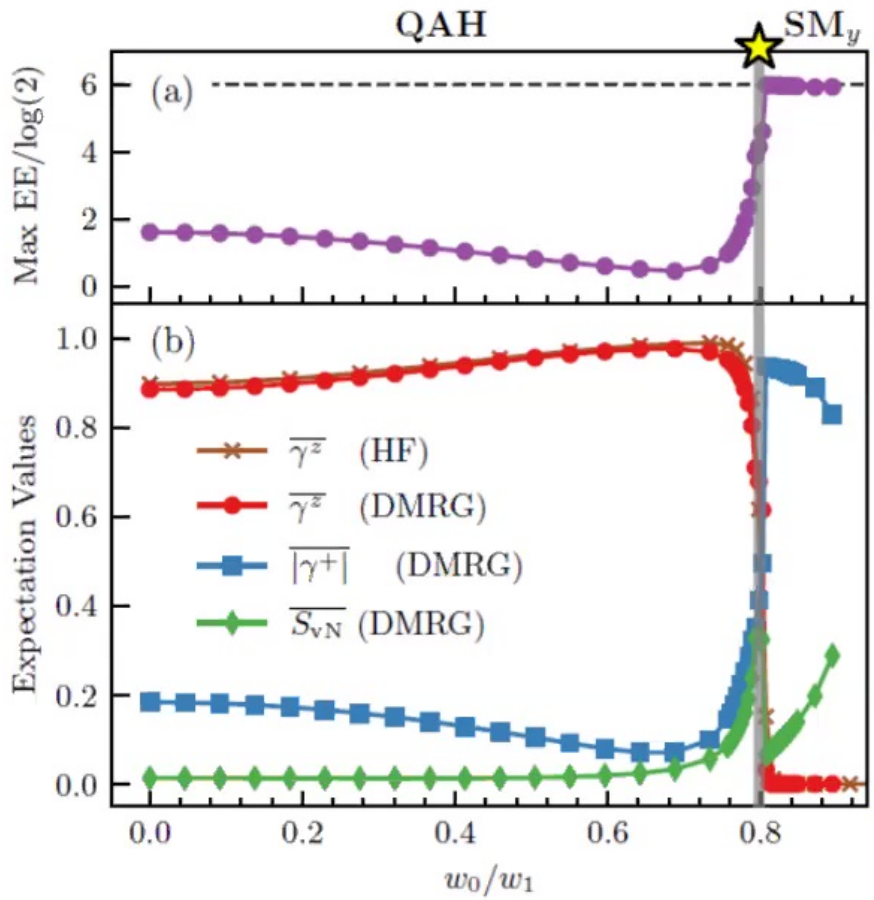

Soejima et al Phys. Rev. B 102, 205111 (2020)

Energetics from a more accurate DMRG algorithm N_y=6 (Zaletel's group)

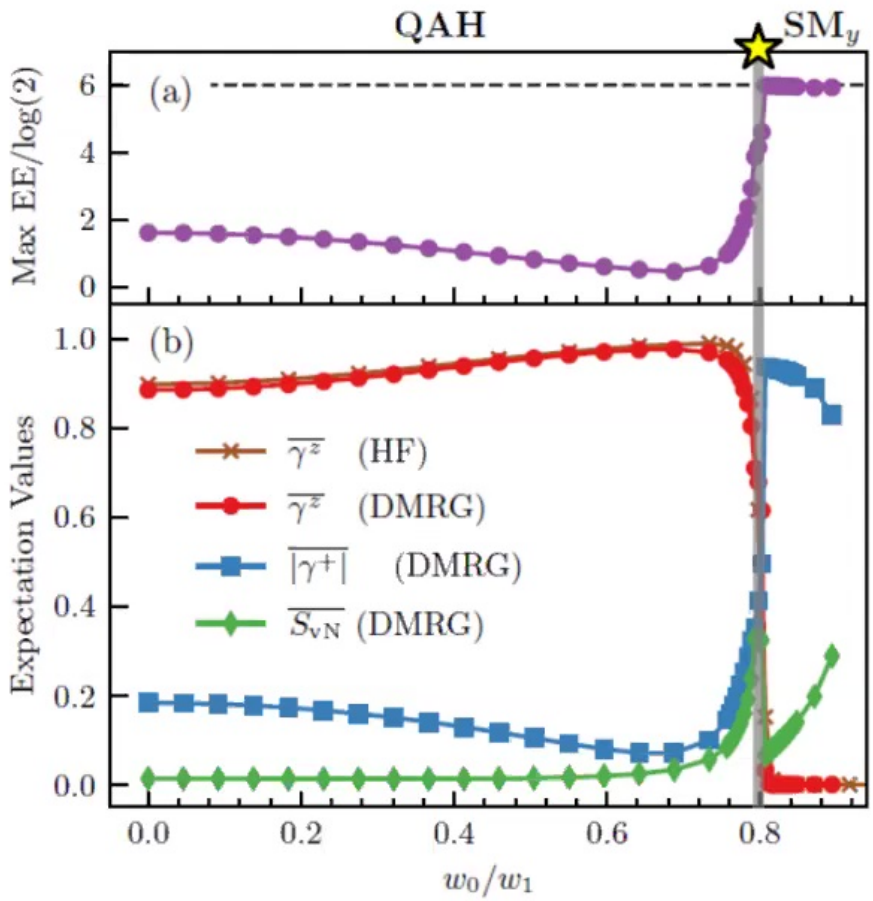

State	Energy (meV)
DMRG ground state (SM$_y$)	−28.24
QAH ansatz [Eq. (14)]	−28.04
SM$_y$ ansatz [Eq. (14)]	−27.92
$C_2\mathcal{T}$ - stripe ansatz [Eq. (14)]	−28.08
Dirac (BM ground state)	−20.62

Advance to the next animation or slide

Soejima et al Phys. Rev. B 102, 205111 (2020)

Experimental indications of period-2 stripe state

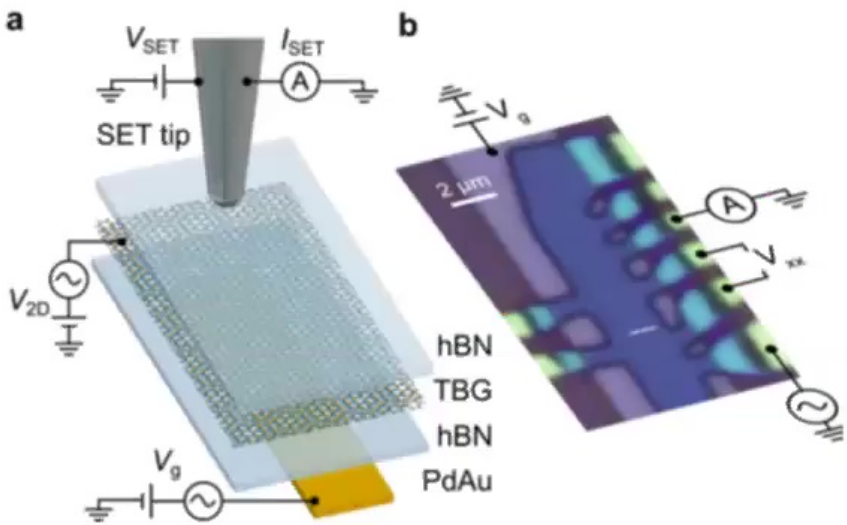

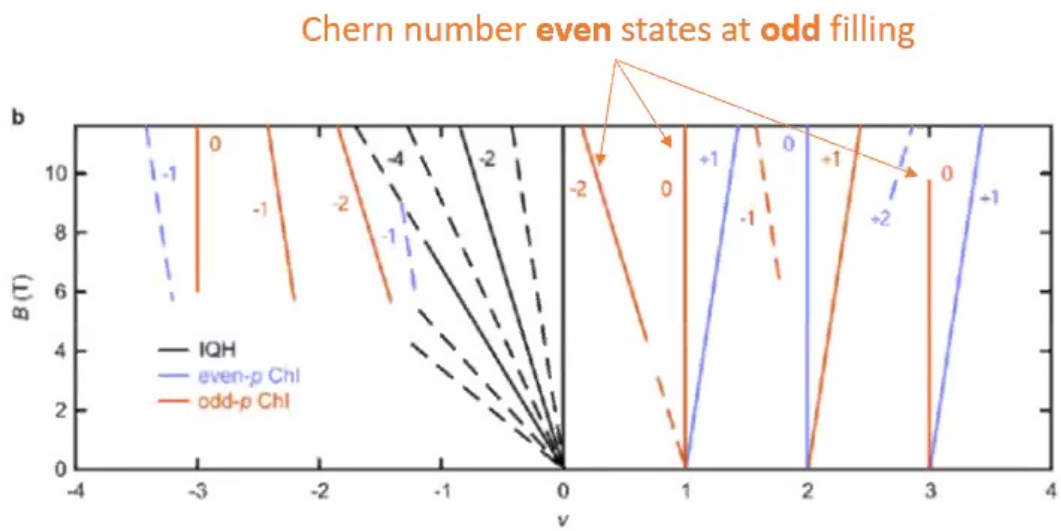

A.T. Pierce et al 2101.04123 (Amir Yacoby and Pablo J-H collaboration)

Exact single particle excitation spectrum in the strong coupling limit: Bloch basis after RG

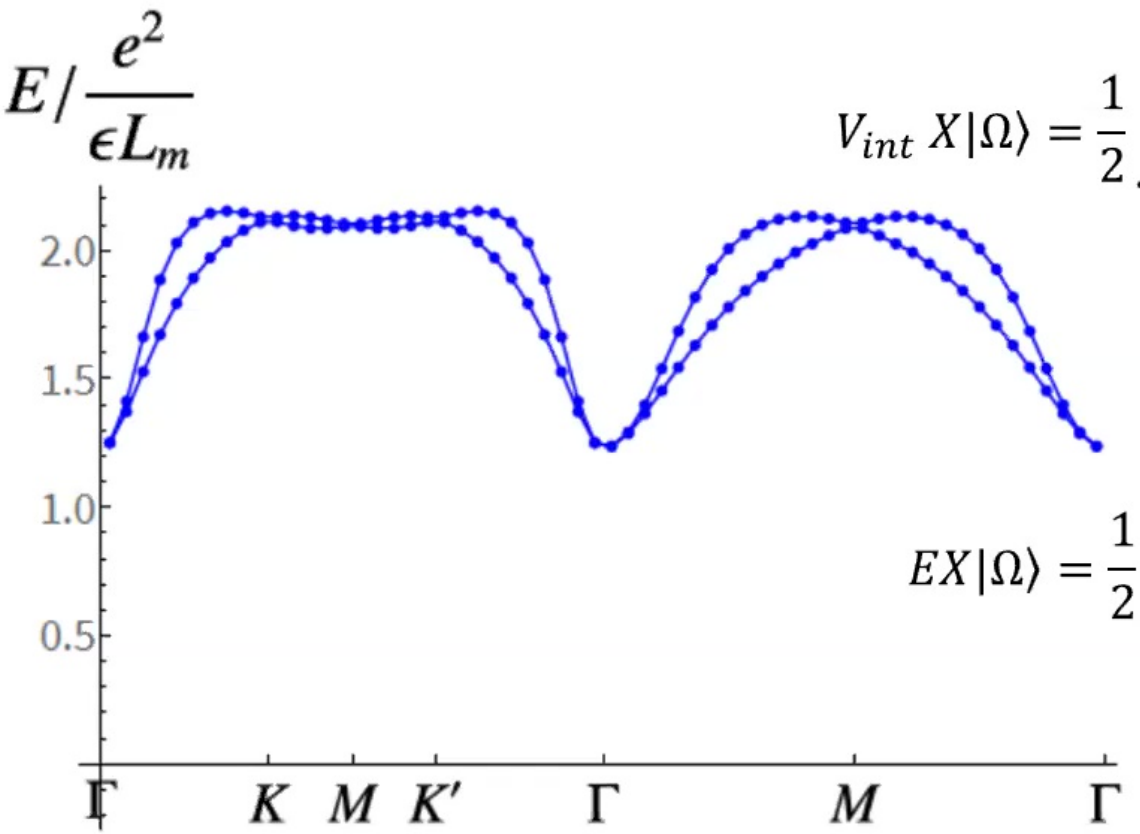

$$V_{int}\, X|\Omega\rangle = \frac{1}{2}\int dr\, dr' V(r-r')\big[\delta\varrho(r),[\delta\varrho(r'),X]\big]|\Omega\rangle$$

$$EX|\Omega\rangle = \frac{1}{2}\int dr\, dr' V(r-r')\big[\delta\varrho(r),[\delta\varrho(r'),X]\big]$$

OV and Jian Kang, PRL 125, 257602 (2020)

Exact (neutral) collective modes in the strong coupling limit: Bloch basis after RG

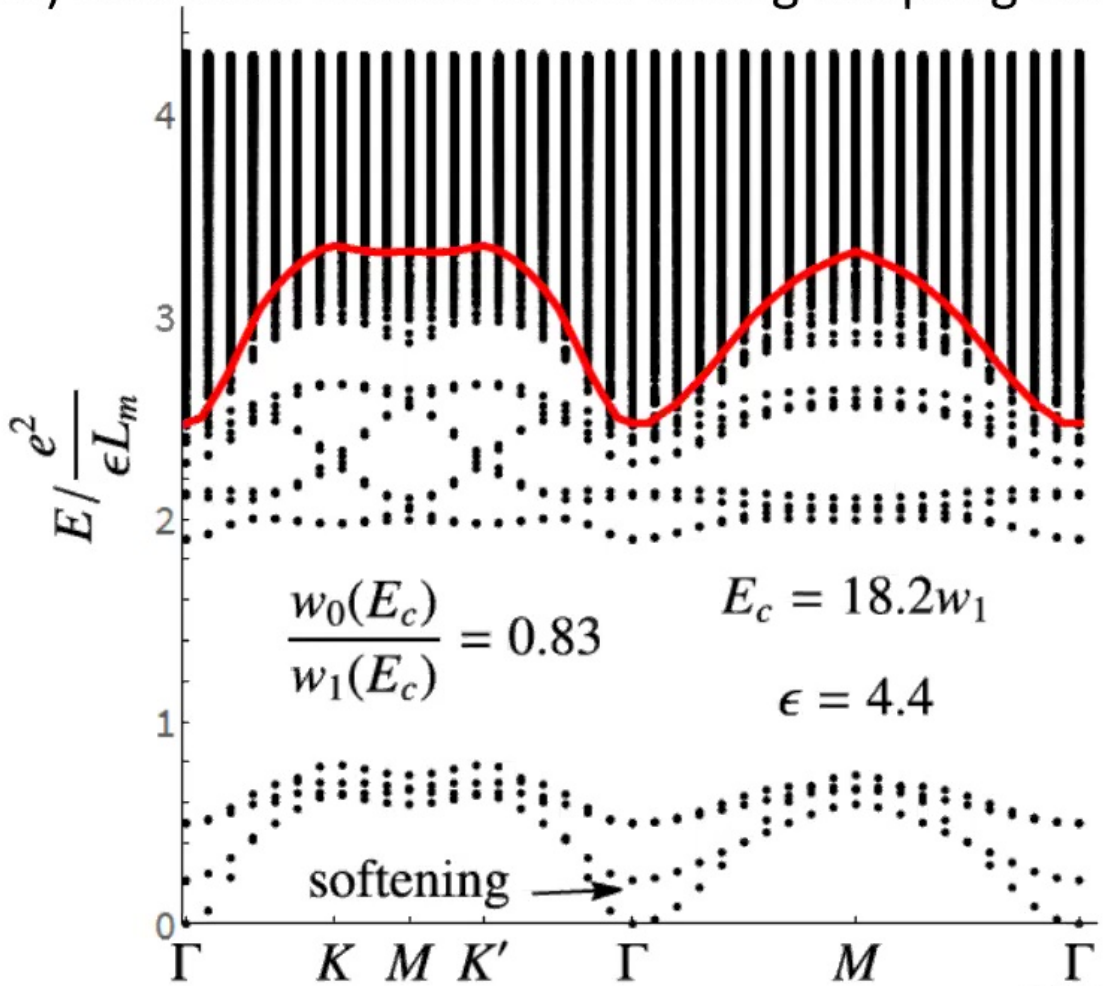

OV and Jian Kang, PRL 125, 257602 (2020)

Justification for the strong coupling approach

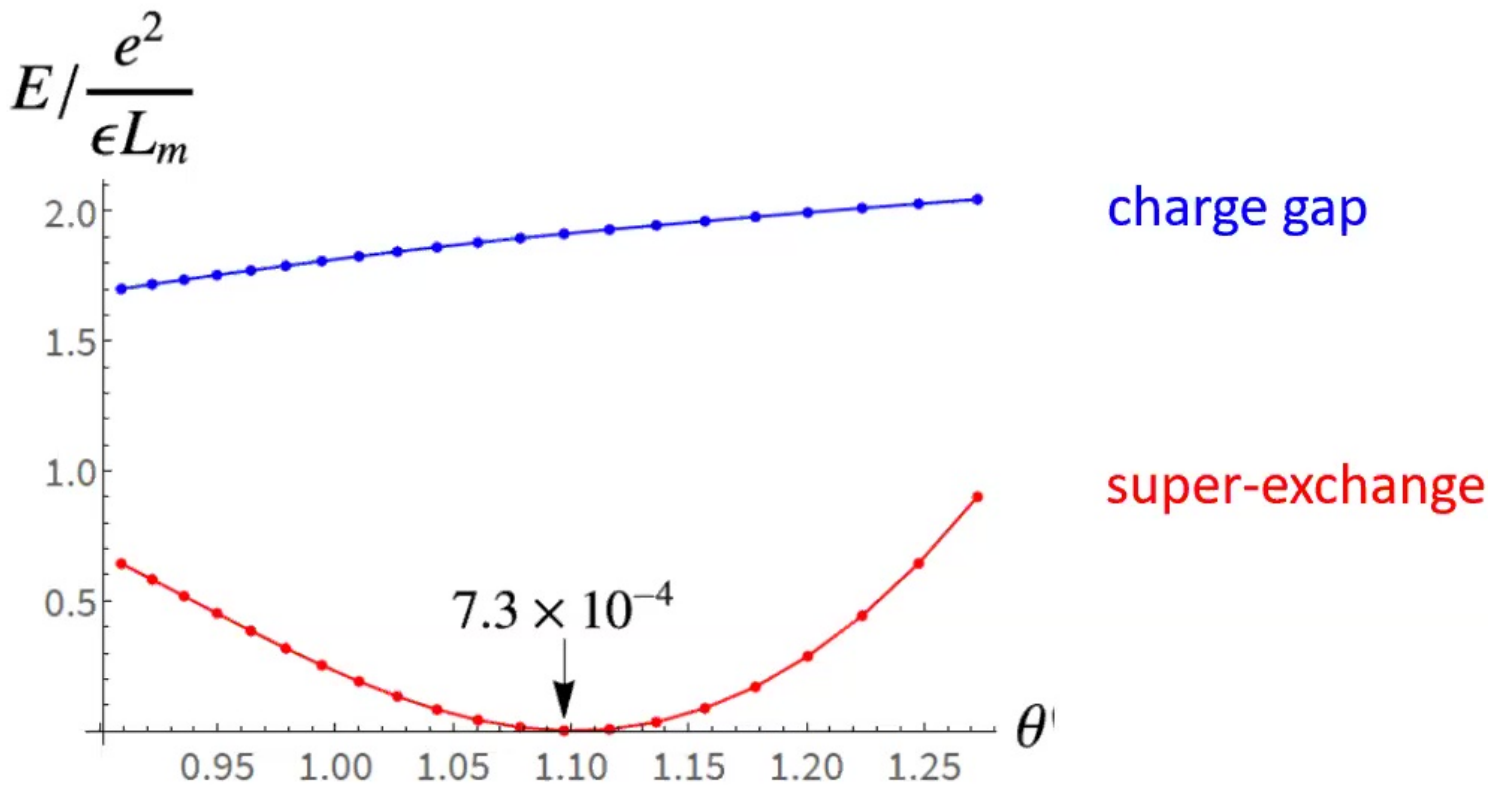

Jian Kang and OV (unpublished)

Summary

- States favored by Coulomb interactions projected onto the basis of the four narrow bands of the magic angle twisted bilayer graphene were presented.

- Due to the unusual shape and symmetry of the 2D Wannier orbitals, the strong coupling problem is qualitatively different from the much studied (topologically) trivial narrow band i.e. a solid in an atomic limit.

- The usual anti-ferromagnetic super-exchange mechanism fails and turns ferromagnetic with an approximate spin-valley SU(4) symmetry.

- Results of DMRG and variational trial state calculations show an approximately product state at odd integer filling and quantum phase transition as a function of a dimensionless parameter.

- The non-Abelian braiding of Dirac nodes was identified as a mechanism for gap opening without C_2T breaking in a stripe state.